

STUDY OF NORMOBARIC HYPEROXIA EFFECTS DURING
FOCAL HYPOXIA- ISCHEMIC INJURY IN MICE USING
OPTICAL SPECTROSCOPY MEASUREMENTS

by

SHEREEN MOHIDEEN

Presented to the Faculty of the Graduate School of
The University of Texas at Arlington in Partial Fulfillment
of the Requirements
for the Degree of

MASTER OF SCIENCE IN BIOMEDICAL ENGINEERING

THE UNIVERSITY OF TEXAS AT ARLINGTON

August 2008

Copyright © by Shereen Mohideen 2008

All Rights Reserved

ACKNOWLEDGEMENTS

I would like to take this opportunity to thank God and my family for their immense support and encouragement throughout my thesis.

I would like to sincerely thank Dr. Hanli Liu for her invaluable guidance and constant support throughout my term in UTA.

I would also like to thank Dr. Steven Kerner for giving me the opportunity to work with him, Dr. Joshua Koch for helping me with the measurements and providing me all the information that was required. I also express my gratitude to Dr. Mario Romero for accepting my request to be a committee member.

Finally, I would like to thank all my lab members and friends, particularly Disha Peswani for her immense support and assistance during all the measurements, Anisha Kaul, Aditya Mathker, Dheerendra Kashyap, Vikrant Sharma and Sweta Narvenkar for their suggestions and cooperation.

July 14, 2008

ABSTRACT

STUDY OF NORMOBARIC HYPEROXIA EFFECTS DURING FOCAL HYPOXIA- ISCHEMIC INJURY IN MICE USING OPTICAL SPECTROSCOPY MEASUREMENTS

Shereen Mohideen, M.S.

The University of Texas at Arlington, 2008

Supervising Professor: Hanli Liu

Optical spectroscopy has seen tremendous growth and development in recent years and has been extensively used to characterize the optical properties of biological tissues. The purpose of this study is to investigate the values of oxygen saturation and concentration of hemoglobin in mice with focal hypoxic ischemia after being recovered in normobaric hyperoxia. Mice at five different age levels were used for this purpose, in order to see the effects of hyperoxia at different developmental stages of the brain; ischemia was induced in them by ligating their right carotid artery and subjecting them to hypoxic (8% oxygen) environment for half an hour. Mice were then subjected to normobaric hyperoxia (100% oxygen) or room air for half an hour. The hyperoxia group showed an increase in oxyhemoglobin concentration in all age groups of mice, also an increase in oxygen saturation was noted in all age groups of mice, except the P28 group. These results indicate that normobaric hyperoxia increases oxyhemoglobin concentration in adult mice with focal cerebral ischemia and the extent of improvement seem to vary with age. This study continues to show the efficiency of optical spectroscopy in determining tissue optical properties, however one of the drawbacks to this

study using needle-like probe was the skin of the animal gave rise to artifacts during measurements and had to be removed to get better optical readings.

TABLE OF CONTENTS

ACKNOWLEDGEMENTS.....	iii
ABSTRACT.....	iv
LIST OF ILLUSTRATIONS.....	viii
LIST OF TABLES	xi
Chapter	Page
1. INTRODUCTION	1
1.1 Stroke	1
1.2 Ischemic stroke.....	2
1.3 The effects of ischemic stroke at the cellular level	3
1.4 Oxygen therapy for stroke	3
1.5 Light tissue interaction	4
1.5.1. Background of optical spectroscopy.....	5
1.5.2. Water	6
1.5.3. Hemoglobin	7
1.6 Research Outline	9
2. MATERIALS & METHODS.....	10
2.1 Experimental Setup	10
2.2 Data Calibration.....	11
2.3 Experimental Protocol	12
3. DATA ANALYSIS.....	15
3.1 Initial data Analysis.....	15
3.2 Effect of the mouse skin on the measurements	17
3.3 Algorithm for oxygen saturation calculation.....	23

4. RESULTS	25
4.1 Results obtained from P7 mice	25
4.2 Results obtained from P14 mice	29
4.3 Results obtained from P21 mice	32
4.4 Results obtained from P28 mice	35
4.5 Results obtained from P60 mice	38
4.6 Age related comparison of HbO and oxygen saturation	40
5. DISCUSSION AND FUTURE WORK	44
REFERENCES	46
BIOGRAPHICAL INFORMATION.....	49

LIST OF ILLUSTRATIONS

Figure	Page
1.1 Schematic illustration of stroke	1
1.2 Absorption spectra of water [9]	7
1.3 Absorption spectra of HbO and Hb [9]	8
2.1 Experimental setup for reflectance measurements from mouse brain tissue	11
2.2 Air tight glass chamber used for 8% oxygen or 100% oxygen delivery to mice	13
3.1 a. Optical reflectance curves obtained from the right side of a P60 mouse during injury and after recovery in normobaric hyperoxia without calibration and normalization , b. Optical reflectance curves obtained from the left side of a P60 mouse during injury and after recovery in normobaric hyperoxia without calibration and normalization	16
3.2a Optical reflectance curves obtained from the right side of a P60 mouse during injury and after recovery in normobaric hyperoxia after calibration and normalization, b. Optical reflectance curves obtained from the left side of a P60 mouse during injury and after recovery in normobaric hyperoxia after calibration and normalization	17
3.3 Experimental setup to study the effect of mouse skin and skull on optical reflectance measurements	18
3.4 Optical reflectance curves obtained using the skin and skull of the first P60 mouse placed on a cuvette filled with deoxygenated blood	19
3.5 Optical reflectance curves obtained using the skin and skull of the first P60 mouse placed on a cuvette filled with oxygenated blood	19
3.6 Optical reflectance curves obtained using the skin and skull of the second P60 mouse placed on a cuvette filled with deoxygenated blood	20
3.7 Optical reflectance curves obtained using the skin and skull of the second P60 mouse placed on a cuvette filled with oxygenated blood	20
3.8 Optical reflectance curves obtained from the first P39 mouse with and without the skin at the site of measurement	22
3.9 Optical reflectance curves obtained from the second P39 mouse with and without the skin at the site of measurement	22
3.10 Illustration of the fitted curve obtained from the optimization algorithm	24

4.1 Concentration of oxy-hemoglobin for P7 mice during hypoxic ischemia and recovery in room air and 100% oxygen	26
4.2 Concentration of de-oxy hemoglobin for P7 mice during hypoxic ischemia and recovery in room air and 100% oxygen	27
4.3 Concentration of Total hemoglobin for P7 mice during hypoxic ischemia and recovery in room air and 100% oxygen	28
4.4 Comparison of oxygen saturation for P7 mice during hypoxic ischemia and recovery in room air and 100% oxygen	28
4.5 Concentration of oxy hemoglobin for P14 mice during hypoxic ischemia and recovery in room air and 100% oxygen	30
4.6 Concentration of de-oxy hemoglobin for P14 mice during hypoxic ischemia and recovery in room air and 100% oxygen	30
4.7 Concentration of total hemoglobin for P14 mice during hypoxic ischemia and recovery in room air and 100% oxygen	31
4.8 Comparison of oxygen saturation for P14 mice during hypoxic ischemia and recovery in room air and 100% oxygen	31
4.9 Concentration of oxy hemoglobin for P21 mice during hypoxic ischemia and recovery in room air and 100% oxygen	33
4.10 Concentration of de-oxy hemoglobin for P21 mice during hypoxic ischemia and recovery in room air and 100% oxygen	33
4.11 Concentration of total hemoglobin for P21 mice during hypoxic ischemia and recovery in room air and 100% oxygen	34
4.12 Comparison of oxygen saturation for P21 mice during hypoxic ischemia and recovery in room air and 100% oxygen	34
4.13 Concentration of oxy hemoglobin for P28 mice during hypoxic ischemia and recovery in room air and 100% oxygen	36
4.14 Concentration of de-oxy hemoglobin for P28 mice during hypoxic ischemia and recovery in room air and 100% oxygen	36
4.15 Concentration of total hemoglobin for P28 mice during hypoxic ischemia and recovery in room air and 100% oxygen	37
4.16 Comparison of oxygen saturation for P28 mice during hypoxic ischemia and recovery in room air and 100% oxygen	37
4.17 Concentration of oxy hemoglobin for P60 mice during hypoxic ischemia and recovery in room air and 100% oxygen	38
4.18 Concentration of de-oxy hemoglobin for P60 mice during hypoxic ischemia and	

recovery in room air and 100% oxygen	39
4.19 Concentration of total hemoglobin for P60 mice during hypoxic ischemia and recovery in room air and 100% oxygen	39
4.20 Comparison of oxygen saturation for P60 mice during hypoxic ischemia and recovery in room air and 100% oxygen	40
4.21 Comparison of oxyhemoglobin concentration on the right (injured) side between all mice in P7, P28 and P60 groups after recovery in room air and 100% oxygen.....	41
4.22 Comparison of oxygen saturation on the right (injured) side between all mice in P7, P28 and P60 groups after recovery in room air and 100% oxygen.....	42
4.23 Comparison of oxyhemoglobin concentration on the right (injured) side between all mice in P14 and P21 groups after recovery in room air and 100% oxygen.....	42
4.24 Comparison of oxygen saturation on the right (injured) side between all mice in P14 and P21 groups after recovery in room air and 100% oxygen.....	43

LIST OF TABLES

Table	Page
2.1 Representing number of mice in each age group	12

CHAPTER 1 INTRODUCTION

1.1 Stroke

Stroke is a disease which affects blood vessels of the brain. It is the third leading cause of death in developed countries following heart disease and cancer [6]. Stroke occurs when a blood vessel carrying oxygen and nutrients to the brain is interrupted by a blood clot, Figure 1.1, or if the vessel itself is ruptured. It is also known as 'brain attack' since it's an acute event and requires immediate treatment. Due to the interrupted blood flow, parts of the brain do not get sufficient amounts of blood and oxygen, which causes brain cells in the affected area to die immediately while damaging others [1]. These damaged cells remain in a compromised state for several hours; hence the time for receiving treatment after stroke plays an essential role in recovery, since dead brain cells cannot be replaced.

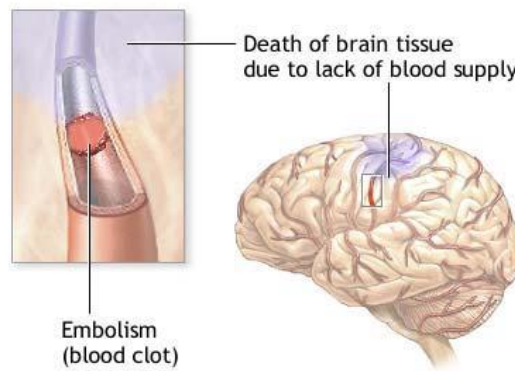


Figure 1.1 Schematic illustration of stroke [2]

The effects of a stroke depend on the type of stroke, the extent of injury and the area of the brain affected. For instance, brain injury from a stroke can give rise to following symptoms: affect in eyesight, motor activity, sense of touch and knowledge of body positioning. It can also cause abnormality in behavior, thought patterns, memory and emotions. Paralysis on one side of the body is common. However, most of these problems can improve and in case of transient ischemic attack symptoms usually disappear within sometime [3].

There are two main types of stroke, namely, hemorrhagic stroke and ischemic stroke. Hemorrhagic stroke occurs when a blood vessel in the brain ruptures and bleeds into surrounding tissues, whereas ischemic stroke is caused by lack of blood flow to the brain [6,7]. It is further explained below.

1.2 Ischemic stroke

Ischemia can be defined as the lack or decrease of blood flow and nutrients to an organ or tissue due to constriction or obstruction of an artery. Brain cells cannot make enough energy to survive from this reduced blood flow causing them to die (infarction), and these dead cells are replaced by fluid-filled cavity (infarct) [4,6].

Several diseases can cause an ischemic stroke, the most common one being atherosclerosis which arises due to cholesterol deposition, which then leads to narrowing of the arteries. Narrowed arteries restrict blood cells to flow, causing them to clot. These clots can hinder the blood flow at the site where they are formed (thrombosis) or can be displaced and moved to an artery closer to the brain (embolism).

Ischemic stroke accounts for 80% of all strokes [5]. It can affect people of all age groups; however it is found to be more common in men than in women [5]. The risk factors for stroke include hypertension, high blood pressure, heart diseases, high blood cholesterol level, diabetes, heavy alcohol consumption, cigarette smoking and drugs like cocaine which causes vasoconstriction, thereby reducing the blood flow [6, 7].

1.3 The effects of ischemic stroke at the cellular level

Reduced blood flow after a stroke causes oxygen decrease in the brain tissue, and this decrease reduces ATP energy production. The cell gets depolarized causing calcium ions to flow into the cell, which in turn results in the rapid increase of intracellular calcium (Ca^{++}) levels. The increase in Ca^{++} ions triggers the release of several glutamate neurotransmitters which in turn stimulate N-methyl-D-aspartate (NMDA) receptors on other neurons. This process results in more influx of calcium into the cells. Excessive calcium in the cells causes it to produce harmful chemicals like free radicals, more glutamate, reactive oxygen species, damaging enzymes, and nitric oxide which further damage and destroy the cell membrane and organelles. The released excessive glutamate, when mitochondria of the cell is destroyed can become neurotoxic, also glycopenia and acidosis may lead to cell apoptosis [9,8,11].

The extent of ischemic injury can be reduced by decreasing the duration of the stroke, which can be possible by intervening with the ischemic cascade mentioned above [9,11]. Several studies for blocking this cascade using neuroprotective agents have been investigated. Investigations for neuroprotection using glutamate antagonists and calcium channel blockers, in an effort to treat stroke, have been done for many years [9]. Only recently neuroprotection for ischemic stroke with the use of a recombinant tissue plasminogen activator called alteplase has been proved to be effective and used in therapy for patients [9]. The timing of restoring blood flow to the tissue after stroke (therapeutic window) plays a critical role in neuronal protection [9].

1.4 Oxygen therapy for stroke

Several treatments are available for stroke; treatment which depend on the severity and type of stroke. Recent studies have proven that oxygen therapy for ischemic stroke can be beneficial. Hyperbaric Oxygen Therapy (HBOT) has been shown to be efficient in various animal and human stroke studies [14]. Studies have shown that HBOT increases oxygen levels in the ischemic region thereby reducing the infarct in the cerebral area by decreasing apoptosis [10]. Treatment using 100% oxygen at a pressure greater than normal atmospheric pressure is

known as HBOT. HBOT increases the concentration of oxygen in all body tissues. When treated regularly it stimulates the growth of new blood vessels (angiogenesis) leading to increase in blood flow at areas affected by ischemia [9,11,12]. HBOT causes the body to be saturated with oxygen giving rise to many therapeutic benefits like killing infections, improving the rate of healing and immune system [13]. The disadvantages of using HBOT include fire hazards (since pure oxygen is used for treatment), not recommended for claustrophobic patients, may cause fatigue, headache, vomiting, the variation in pressure in the treatment chamber can cause damage to the ear, sinus and even the lungs [14]. Along with the above mentioned disadvantages, the limited availability of hyperbaric chambers and negative results of few HBOT studies have given rise to alternate means of oxygen therapy for ischemic stroke [38]. (No significant improvement between treatment in air and hyperbaric oxygen therapy, in treatment of human stroke was seen in study of HBOT [15], another study of HBOT for patients with acute ischemic stroke, at a pressure level of 2.5 ATA for 60 minutes was also proven to be ineffective and maybe even harmful [16]). Normobaric hyperoxia when compared to HBOT has lesser potential side effects when administered for less than 24 hours; it is inexpensive, more available, no pressure chamber is required, slows down the process of infarction and allows for treatment of the patient within minutes after a stroke by emergency medical staff [37,38]. This technique of administering 100% oxygen at normal atmospheric pressure is considered a potential therapy to save damaged tissue after ischemic stroke and is under investigation in several recent studies [37,38].

In this study the impact of normobaric hyperoxia on concentrations of oxyhemoglobin and deoxyhemoglobin were calculated using optical spectroscopy measurements, the principle and theory of these measurements are described below.

1.5 Light tissue interaction

Light traveling through a biological tissue can undergo either absorption or scattering by particles present in the tissue. The size, shape, mismatch of refractive indices and the density of

the scatters in the tissue are the important factors that influence the tissue optical properties. Light absorption in the tissue is determined by the concentration of the chromophores (light absorbing particles within tissue) present, and is a function of the wavelength. Major chromophores which absorb light in living tissues are oxygenated hemoglobin (HbO) and deoxygenated hemoglobin (Hb) molecules, myoglobin, water, melanin and other tissue chromophores each of which has its own unique optical absorption spectrum in the visible and NIR region [17].

1.5.1. Background of Optical Spectroscopy

Optical spectroscopy is a well established technique used for measuring tissue oxygenation, hemoglobin concentration and hemoglobin oxygen saturation. Optical spectroscopy measurements can be done using optical probes with small source-detector separation, and this method is preferred due to its low risk, low cost and minimally invasive way to study various properties of tissues and organs.

Near infrared spectroscopy (NIRS) is based on the principle that near infrared light (700 to 1100nm) can pass through tissue and be scattered, absorbed (by blood chromophores like oxyhemoglobin and deoxyhemoglobin) and transmitted [18,19]. Changes in amplitude of the detected light, after it has followed the 'banana' pattern within the tissue, can provide information about changes in chromophore concentration [18,20]. This principle is used in various studies for quantification of hemoglobin concentration, oxygen saturation etc. Studies have shown that the depth of penetration of near infrared (NIR) light in NIRS, increases with increase in separation between the source and detector [19,21]. Since, the light source and detector used for NIRS study must be at least few centimeters or more apart, in order to pass deep into the tissue it was not used in this study [21,22]. Measurements done for this study required readings from both the left (normal) and right (injured) side of the mouse brain, and placing an NIRS probe with a source detector separation in the range of few centimeters was not possible due to the small size of the mouse brain. Also, hemoglobin absorbance in the NIR range Figure 1.3 is relatively weak when compared to its absorbance between the wavelength

range of 400-700nm [21]. Studies evaluating the ability of visible light spectroscopy show that it can be used for evaluating the concentrations of chromophores and detect ischemia in both human and animal subjects [23,24]

The wavelength range considered for this optical spectroscopy study was between 400nm-700nm (visible light spectroscopy). The measurements for this study are performed on mice, with the optical probe placed on the skull of the animal. Since the thickness of the skull is less than 1mm light penetrates deep enough into the tissue to provide sufficient information.

The optical spectroscopy measurements are based on the principle of Beer-Lambert law which gives an empirical relationship relating the absorption of light to the properties of the material through which the light travels [9]. It can be represented as follows:

$$A = \text{Log} (I_0/I) = \epsilon cd \quad \text{----- equation (1)}$$

When light travels a distance 'd' through a medium consisting of an absorbing compound (chromophore) of concentration 'c', then the intensity of the transmitted light (I) is less than the intensity of the incident light (I_0), since some of the light travelling through the medium is absorbed. This reduction or loss of light known as the attenuation 'A' measured in units of optical density (OD) is equal to the logarithm of I_0/I . 'ε' is the specific absorption coefficient of the chromophore given in ($\text{molar}^{-1}.\text{cm}^{-1}$). The product of ϵc is known as the extinction coefficient of the absorbing medium.

Using natural logs equation (1) is rewritten as $I = I_0 e^{-\alpha cd}$ where 'α' is the absorption per mole of compound per centimeter of optical path, and is given as (μ_a/c). 'μ_a' is the absorption coefficient (cm^{-1}) and is described as the probability that a photon will be absorbed by the medium it travels through per unit length [25].

1.5.2. Water

Water is the most abundant chemical substance in the human body. It accounts for 60 to 80% of the total body mass; the content differs with tissue type, gender and age. Due to the high concentration of water in tissue, it is considered an important chromophore in tissue spectroscopy measurements [26]. The absorption spectrum of water is shown below Figure 1.2.

Between 400 and 900nm water shows a region of relatively low absorption, and above 900nm the absorption coefficient increases rapidly to a peak at around 970nm. Water absorption is more prominent at wavelengths above 900nm. Hence the water absorption spectrum is said to exhibit a 'window' of transparency in the wavelength range of 200-900nm within which spectroscopy measurements are made [25, 26].

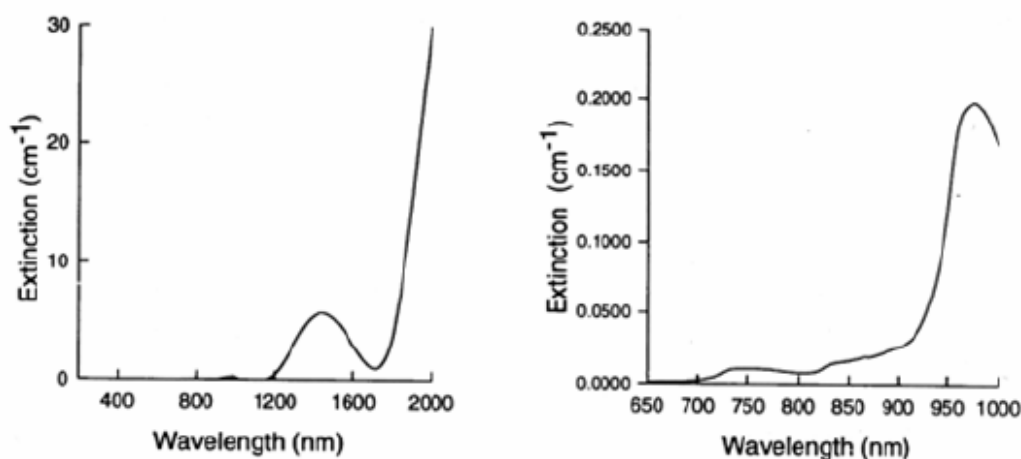


Figure 1.2 Absorption spectra of water. Left: Absorption spectrum over wavelength range 400-2000nm. Right: Absorption spectrum on an expanded scale from 650-1000nm (NIR wavelength range) [26]

1.5.3. Hemoglobin

Hemoglobin is the protein molecule in red blood cells which delivers oxygen from the lungs to the tissues, and returns carbon dioxide from the tissues to the lungs. It consists of four polypeptide subunits; each subunit has a haem group. Each haem group contains an iron atom which has the ability to bind to oxygen to become oxygenated hemoglobin (HbO). One hemoglobin molecule therefore can carry four molecules of oxygen. Hemoglobin molecule is known as deoxyhemoglobin (Hb) when no oxygen molecules are attached to it. The absorption spectra of HbO and Hb are shown in Figure 1.3.

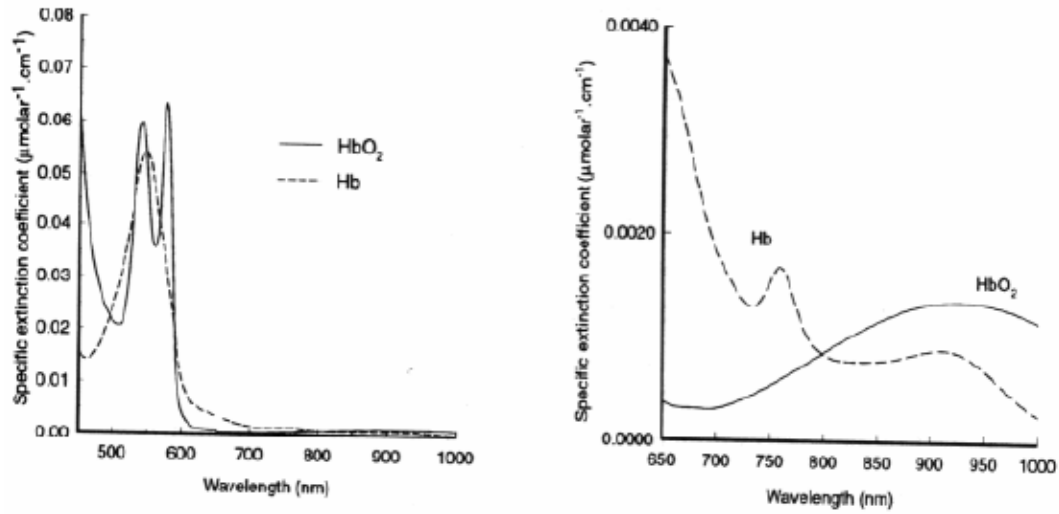


Figure 1.3 Absorption spectra of HbO and Hb. Left: Absorption spectrum over the wavelength range 500-1000nm. Right: Absorption spectrum in the NIR region. [26]

It can be clearly seen that the absorption spectra of HbO and Hb shown above differ significantly. When compared to water, HbO and Hb show significant absorption below the 650nm wavelength range. These characteristics of hemoglobin absorption are used for spectroscopic measurements in this study.

When compared to hemoglobin, myoglobin has a very low sensitivity to tissue oxygenation although it has an absorption spectrum similar to that of hemoglobin. Moreover, myoglobin is found only within the cells of skeletal and cardiac muscles and therefore can be excluded from our studies, since this study primarily deals with the brain tissue.

Scattering of light in tissues occurs due to heterogeneity in the refractive index at the boundaries of different media. The cell membrane and the membranes of organelles present inside the cell (regarded as solid contents of tissue) cause the light to scatter. Red blood cells make up for about 2 percent of the solid contents of tissue, hence the attenuation of light due to these cells is considered to be low [27].

1.6 Research Outline

It is not known if normobaric hyperoxia considerably impacts oxygen delivery to the ischemic tissue and if normobaric hyperoxia can cause vasoconstriction in the ischemic tissue during recovery. The main aim of my study was to address these questions by using the technique of optical spectroscopy to investigate the effects of normobaric hyperoxia during focal hypoxia ischemic injury in mice of different age groups on both the injured side and the normal (control) side of the brain, and also to compare the recovery of mice breathing in 100% oxygen (normobaric hyperoxia) with that of mice breathing in room air. In the following pages the protocol for this experiment, the experimental setup and the results acquired from the mice measurements are discussed. Initial analysis of the acquired data shows a significant difference between optical spectra of the injured and normal tissue demonstrating that this technique of optical spectroscopy measurements is effective in distinguishing between healthy and ischemic tissue. Further, quantification of concentrations of oxyhemoglobin, deoxyhemoglobin, total hemoglobin and the percentage of oxygen saturation of the tissues measured were determined using optimization algorithm technique [28,29].

CHAPTER 2

MATERIALS & METHODS

2.1 Experimental Setup

This study was performed using a tungsten-halogen light source (HL-2000, Ocean Optics, Inc., Dunedin, FL), a needle-like probe, spectrometer (USB 2000, Ocean Optics, Inc., Dunedin, FL) and a laptop computer with OOI Base32 software (Ocean Optics, Inc., Dunedin, FL) as shown in Figure 2.1.

Light in the 400-700 nm wavelength range is passed through the light-delivery fiber to the optical probe which has a small source-detector separation (referred to as needle-like probe). Before the measurement, a small portion of the mouse skin above the skull is removed, shown in Figure 2.1 in order to decrease artifacts due to the skin; measurements are done on the mouse skull. The probe is placed in contact with the mouse skull surface, without much pressure, to deliver light into it. The fiber optic probe has a diameter of about 2 mm and contains one light delivery fiber and one light-collection fiber. Each fiber is 200 μ m in diameter. The reflected light from the mouse is collected by the probe with the light-collection fiber and transmitted to the real-time display spectrometer which converts the optical signal into an electrical signal. The output signal from the spectrometer is saved in the laptop using the software.

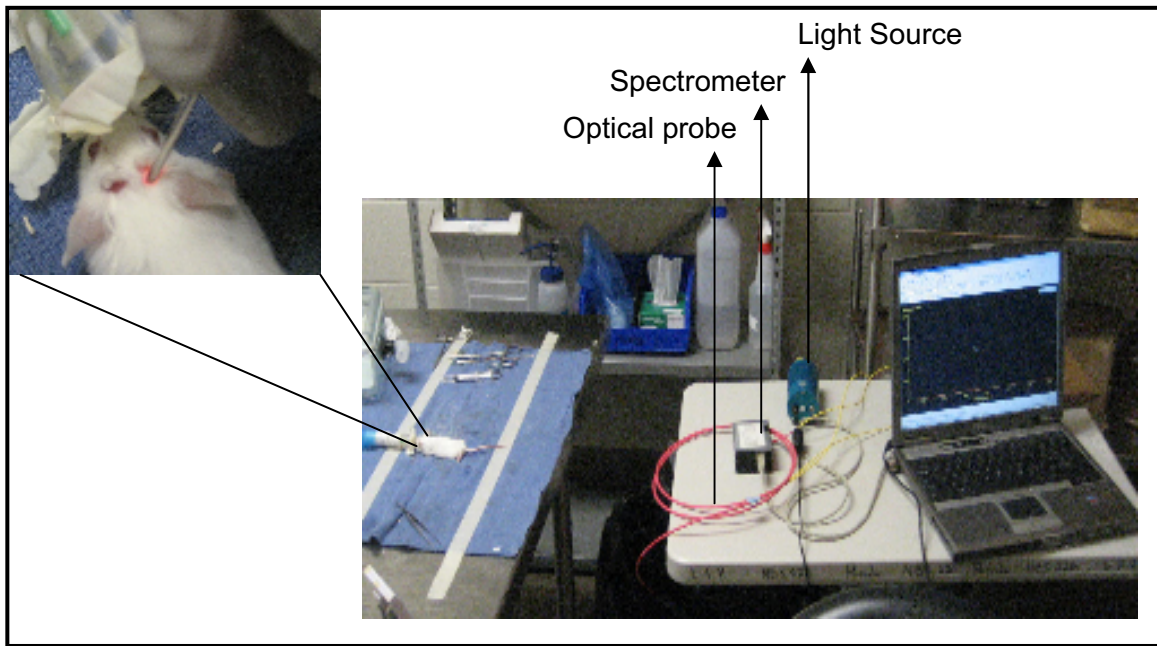


Figure 2.1 Experimental setup for reflectance measurements from mouse brain tissue

2.2 Data Calibration

In order to get the chromophore concentration from the least square fitting algorithm, the measured raw reflectance data has to be calibrated. Calibration was done using the optical spectral readings obtained from a white reference sample (Diffuse reflectance sample, Ocean Optics, Inc., FL). The white sample provides reflectance $>99\%$ in the wavelength range of 250-2500nm. Hence dividing the measured reflectance curve (obtained from the mouse) by the calibration curve (obtained from the white reference sample) gives the spectral effects of only the tissue being studied, excluding any other spectral effects from the light source, optical fibers etc.

2.3 Experimental Protocol

This study includes measurements from 5 different age groups of mice. The total number of mice in each group, including the number of mice recovered in room air and normobaric hyperoxia (100% oxygen) are given below.

Table 2.1 Representing number of mice in each age group

Age	Total Number (n)	Recovered in Room Air	Recovered in 100% oxygen
7 days (P7)	9	3	5
14 days (P14)	9	5	4
21 days (P21)	10	5	5
28 days (P28)	6	3	3
60 days (P60)	15	7	8

Mice at five different age levels were used for this study, to investigate the effects of hyperoxia at different developmental stages of the brain. The brain of a p7 mouse is thought to be as mature as a third trimester human fetus [30, 11] and that of p14 and p21 to infants, and p28, p60 compared to a more developed brain tissue. Focal cerebral hypoxia-ischemia was induced in all mice ready for measurements following the Rice Vannucci model, which involves the ligation of the common carotid artery followed by the exposure to a hypoxic atmosphere.

In this experiment, the right common carotid artery was ligated in all the mice used. The carotid artery was ligated using a surgical silk thread. These mice were then placed aside for a recovery period of about 2 hours. The mice were divided into 2 groups, one group for recovery in room air and the other for recovery in 100% oxygen (hyperoxia). For instance, P21 had a total number of 10 mice, 5 mice were recovered in room air after the injury and 5 mice were recovered in hyperoxia. Ligation of the carotid artery does not cause ischemia in the mouse, but

placing them in hypoxia (8% oxygen) after the ligation causes the ischemic injury [31]. Hence, after the recovery period, mice were placed in an air tight glass chamber as shown in Figure 2.2, where they were exposed to 8% oxygen under normal atmospheric pressure (normobaric-hypoxic atmosphere) for half an hour. Each mouse was then taken out of the chamber and anaesthetized with isoflurane. A small portion of the skin was cut at the site of measurement, in order to avoid artifacts from the skin and the probe was placed on the skull. At first the dark background measurement was recorded with the same settings but with the light source switched off. This is done in order to subtract the background data from each of the measured reflectance spectrum so that any noise from the background can be eliminated. After the background measurement, the reflectance was measured from the right side of the brain, followed by measurement on the left side. The mouse was then placed in a cage, and let to recover in room air for half an hour. After recovery in room air, the mice were anaesthetized again using isoflurane and measurements were recorded from the right and left side of the brain.

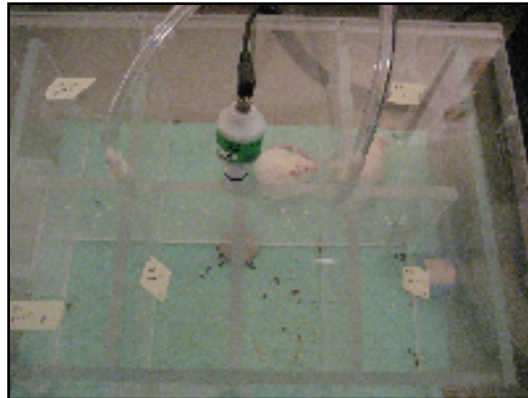


Figure 2.2 Air tight glass chamber used for 8% oxygen or 100% oxygen delivery to mice

Similarly for the group of mice which had to be recovered in hyperoxia, initially they were placed in the normobaric-hypoxic chamber for half an hour after which they were anaesthetized, a small portion of their skin was cut and the reflectance measurements were recorded on the right and left side of the brain. Then the mice were placed in an air tight

chamber and exposed to 100% oxygen (normobaric hyperoxia) for half an hour followed by reflectance measurements on the right and left side of the brain.

All measurements were taken at an integration time of 40ms. This protocol was followed for all mice measurements. The skin was removed in all mice except the P14 and P21 group.

CHAPTER 3

DATA ANALYSIS

3.1 Initial data Analysis

As mentioned earlier, after subtracting the dark background reflectance measurement from the data we calibrated using the reflectance spectrum from the white sample. Then the data was normalized at 500nm wavelength, to check for the absorption curve due to hemoglobin and compare reflectance spectra before and after injury. The raw data is shown in Figure 3.1(a) and (b) and the data after calibration is shown in Figure 3.2(a) and (b). The calibrated data between 500 to 600nm wavelength range (visible region) highlight the spectral characteristics of hemoglobin. The 'w' shape is a qualitative indicator of oxygen saturation percentage. The depth of the 'w' shape increases as the saturation value increases, which represents a higher concentration of HbO. Increase in Hb concentration is indicated by a shallow 'w' shape or a 'v' shape in the visible region, thereby representing a lower oxygen saturation percentage [32]. These characteristics of HbO and Hb were evident in the recorded data. Figure 3.2 shows the optical reflectance measured in a P60 mouse on the right side of the brain during injury (hypoxia) and during recovery period (hyperoxia). It is clearly seen that during injury the concentration of HbO is less when compared to its concentration during recovery. This is inferred with respect to the spectral characteristics of hemoglobin molecules.

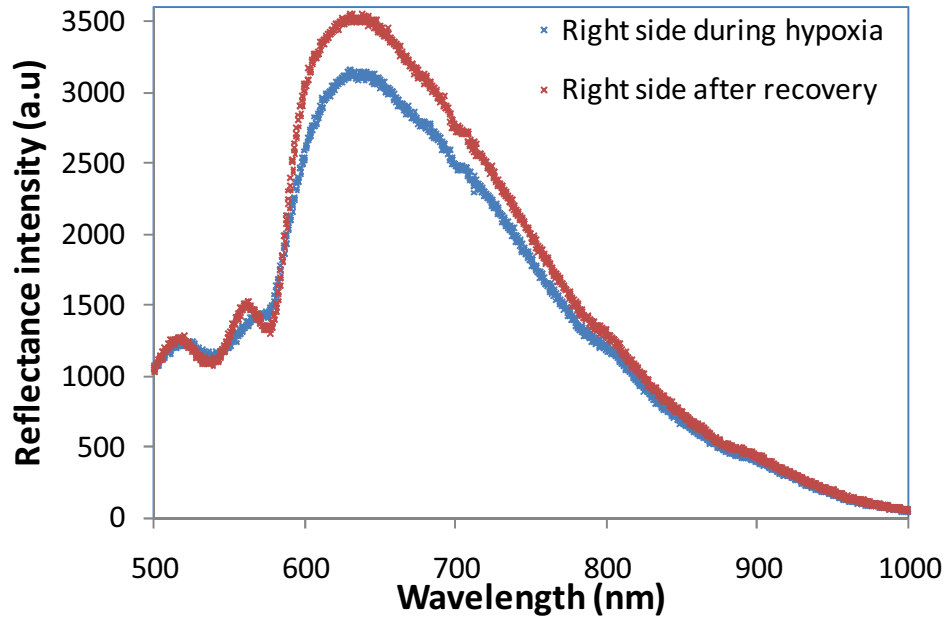


Figure 3.1(a) Optical reflectance curves obtained from the right side of a P60 mouse during injury and after recovery in normobaric hyperoxia without calibration and normalization

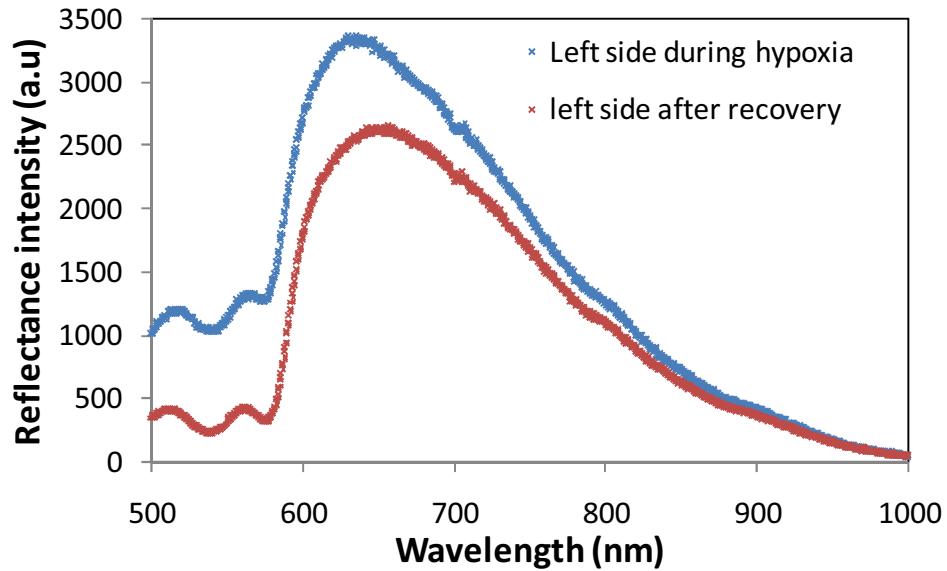


Figure 3.1(b) Optical reflectance curves obtained from the left side of a P60 mouse during injury and after recovery in normobaric hyperoxia without calibration and normalization

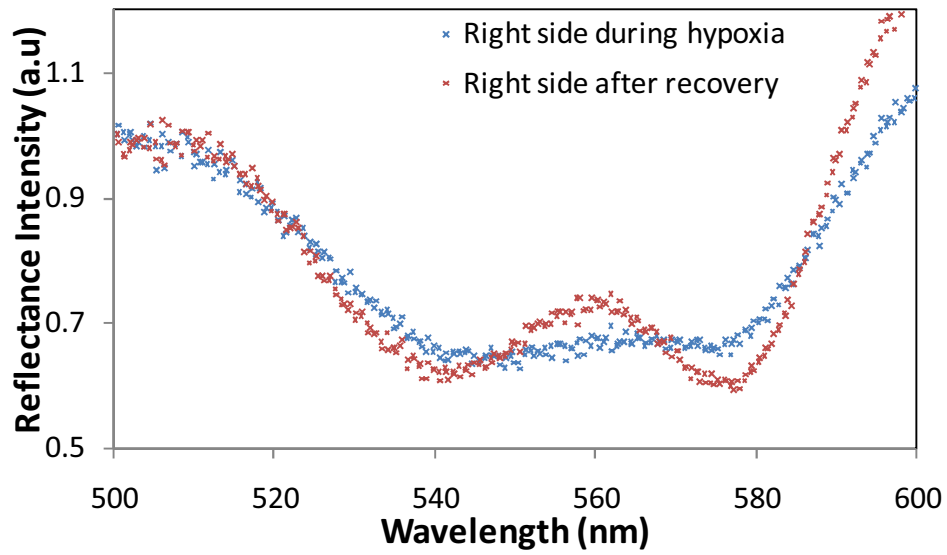


Figure 3.2(a) Optical reflectance curves obtained from the right side of a P60 mouse during injury and after recovery in normobaric hyperoxia after calibration and normalization

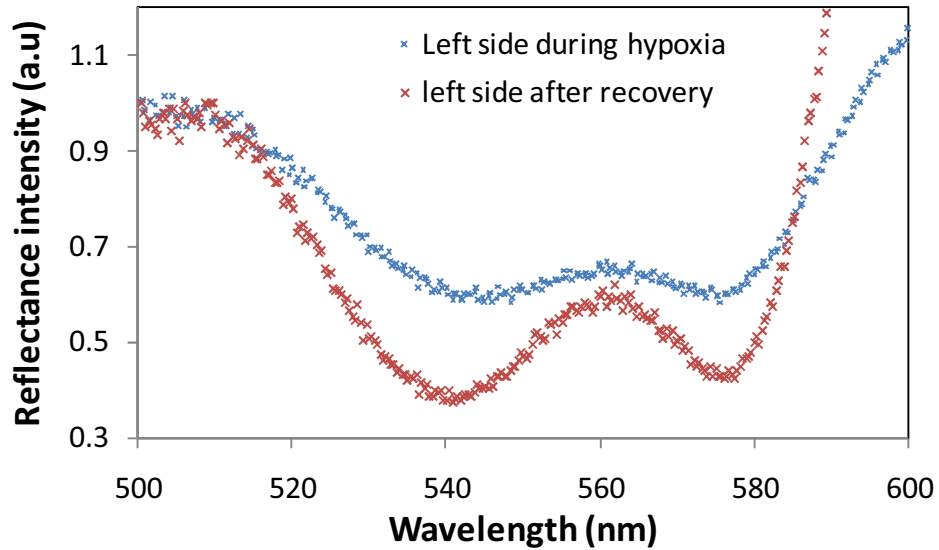


Figure 3.2(b) Optical reflectance curves obtained from the left side of a P60 mouse during injury and after recovery in normobaric hyperoxia after calibration and normalization

3.2 Effect of the mouse skin on the measurements

Initially measurements for this study were recorded from the mouse without cutting its skin. Measurements were taken after shaving the mouse skin and placing the optical probe directly on skin at the site of measurement. Analysis of the data obtained from this manner of measurement showed a significant decrease in signal intensity and also the characteristic 'w'

shape of hemoglobin was not clearly evident. In order to see how the measured signal was being affected by the skin and/or the skull the following experiments were performed using a small piece of the skin and skull. This measurement was done using the skin and skull of two P60 mice, two cuvettes, the first cuvette filled with highly oxygenated blood-intralipid solution and the second filled with highly deoxygenated blood-intralipid solution in an effort get the reflectance properties similar to that of the mouse tissue when healthy and injured. Defibrinated horse blood mixed with intralipid solution was used and the percentage of oxygen saturation was measured using the ISS oximeter. Initially the reflectance was measured from the first cuvette alone by placing the optical probe directly on it. Then, only the mouse skin is placed on the cuvette and reflectance measurement is recorded, similarly only the mouse skull is placed on the cuvette and reflectance is measured followed by reflectance measurement by placing both the skin and the skull (one on top of the other) on the cuvette as shown in Figure 3.3. This procedure is repeated with the second cuvette containing deoxygenated blood-intralipid solution. The reflectance data obtained is calibrated and normalized.

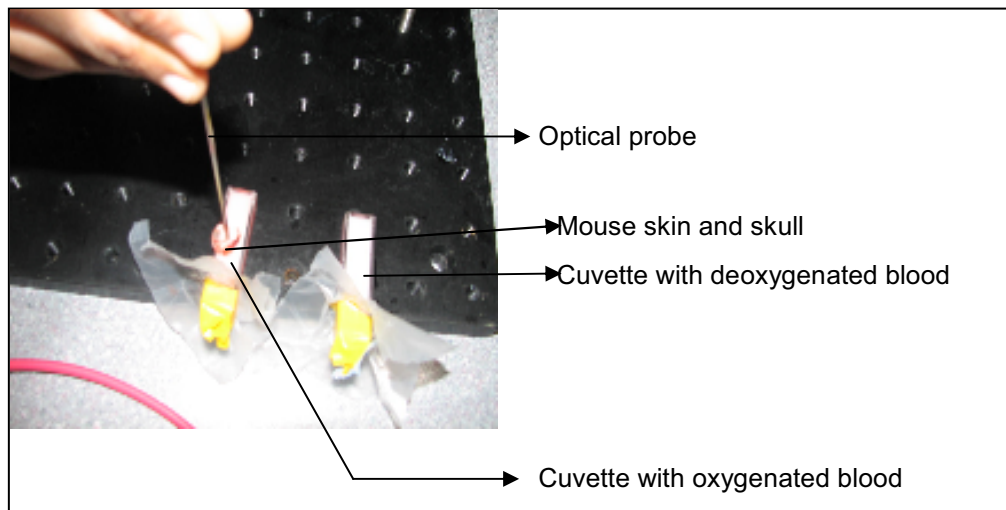


Figure 3.3 Experimental setup to study the effect of mouse skin and skull on optical reflectance measurements

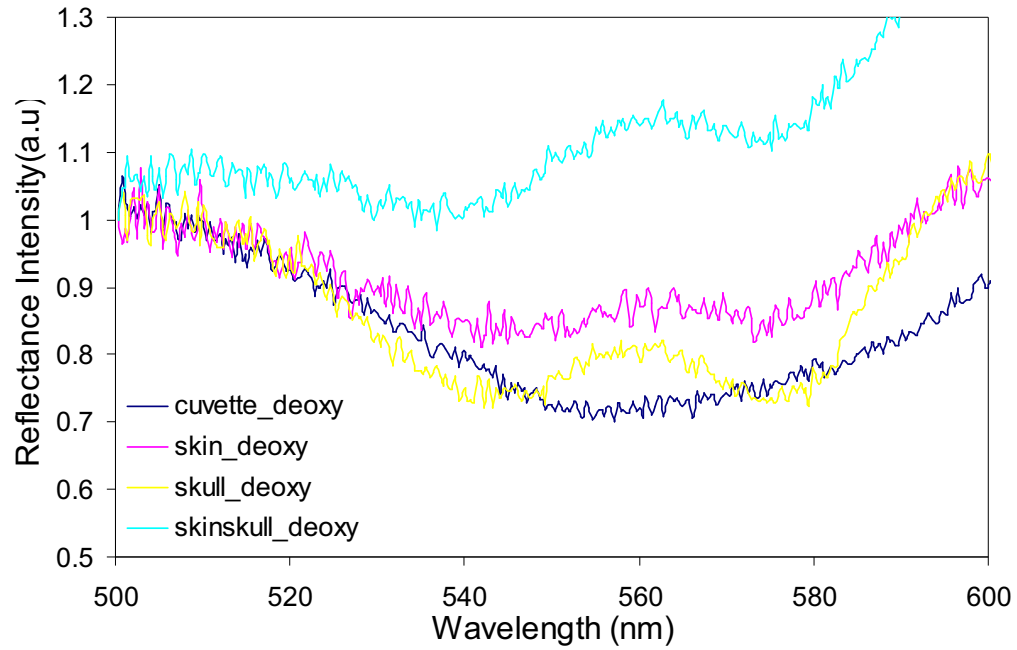


Figure 3.4 Optical reflectance curves obtained using the skin and skull of the first P60 mouse placed on a cuvette filled with deoxygenated blood

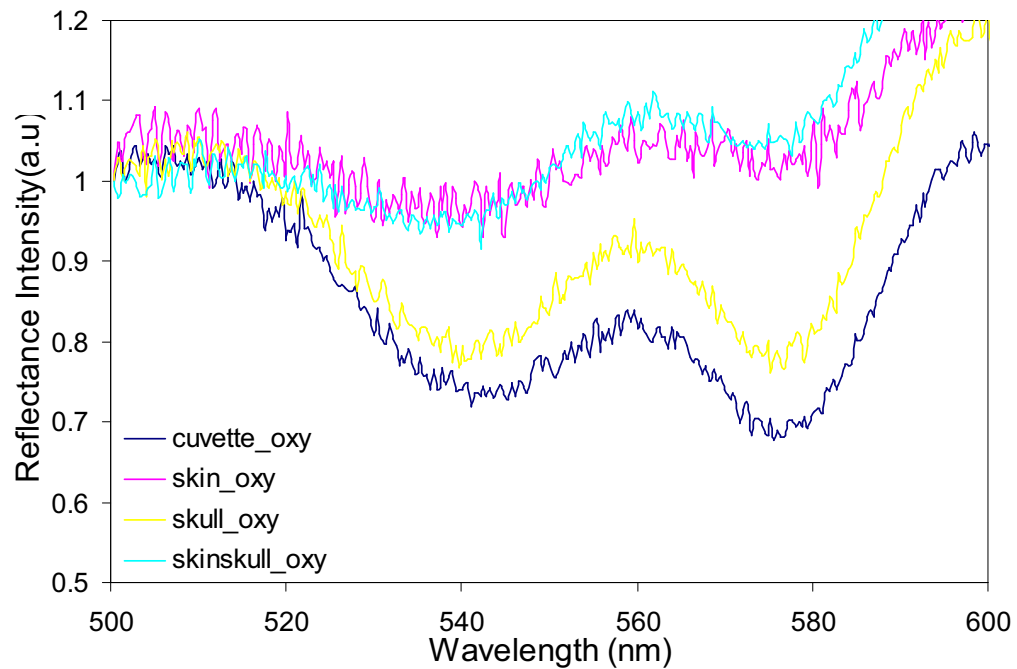


Figure 3.5 Optical reflectance curves obtained using the skin and skull of the first P60 mouse placed on a cuvette filled with oxygenated blood

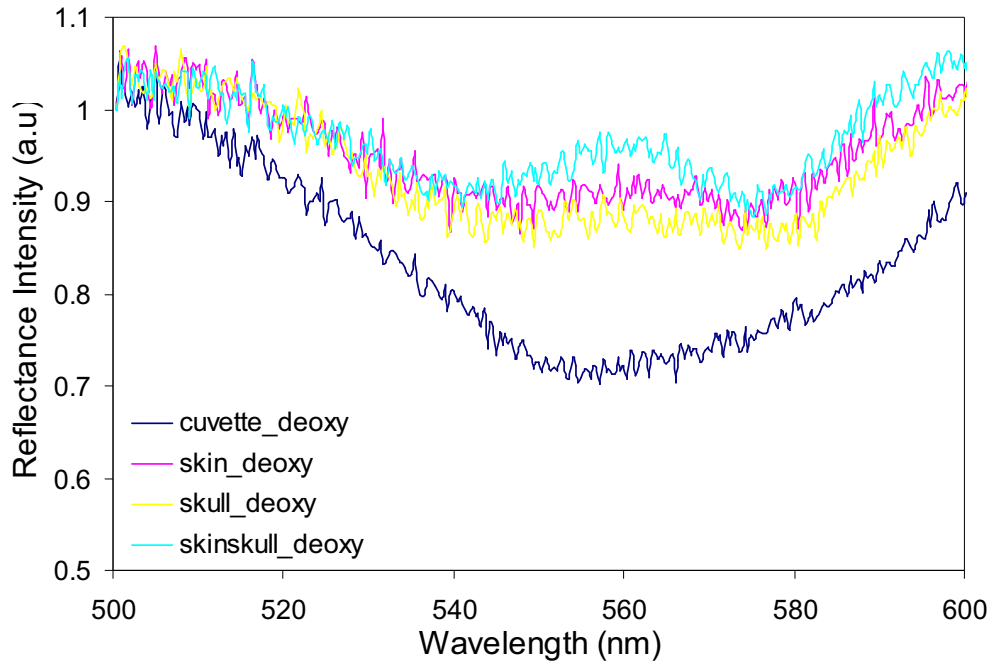


Figure 3.6 Optical reflectance curves obtained using the skin and skull of the second P60 mouse placed on a cuvette filled with deoxygenated blood

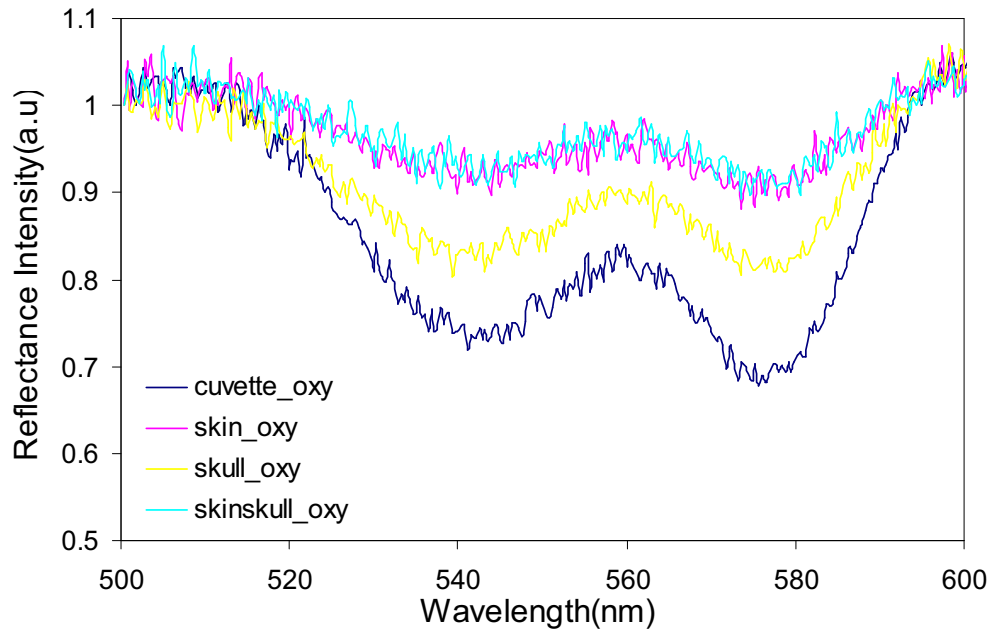


Figure 3.7 Optical reflectance curves obtained using the skin and skull of the second P60 mouse placed on a cuvette filled with oxygenated blood

Figure 3.4 and 3.5 shows the optical reflectance measured using the skin and skull of the first mouse on the cuvette filled with deoxygenated blood and the cuvette filled with oxygenated blood respectively. Similarly figure 3.6 and 3.7 shows the optical reflectance measured using the skin and skull of the second mouse on the cuvette filled with deoxygenated blood and the cuvette filled with oxygenated blood respectively. From the above plots it is clear that the original reflectance intensity of the cuvettes is altered by the skin. It can be seen that measurements from the cuvette with oxygenated blood-intralipid solution show a clear 'w' shape indicating higher concentrations of oxygenated hemoglobin, and readings after placing the skin alone on the cuvette gives a shallow 'w' shape which represents higher deoxygenated level though that was not the case. This proved that the mouse skin gave rise to artifacts. Readings after placing the skull alone on the cuvette also altered the reflectance measurements from the cuvette, but it was less when compared to that of the skin. The skull could not be removed without damaging the tissue below it, hence the skull of the animal was kept intact during all the measurements.

To confirm the effect of the skin on the reflectance intensity, measurements of the reflectance intensity from two normal P39 mice were taken, by initially placing the optical probe on the mouse head without removing the skin. Measurements were recorded from both left and right side of the head. Then the skin was removed at the site of measurement and readings were taken on the skull. The results Figure 3.8 and Figure 3.9 were similar to that of the above experiment with the cuvette. The mouse skin altered the reflectance intensity; the optical signal measured after removing the mouse skin showed better hemoglobin absorption spectra characteristics. Hence, the skin of the mouse was removed during measurements to reduce the artifacts.

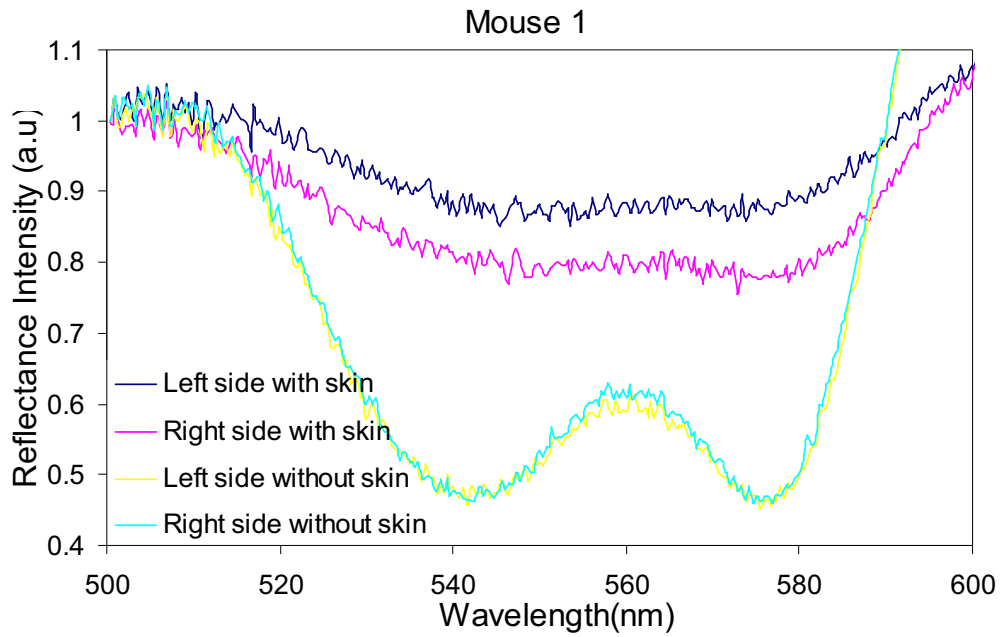


Figure 3.8 Optical reflectance curves obtained from the first P39 mouse with and without the skin at the site of measurement

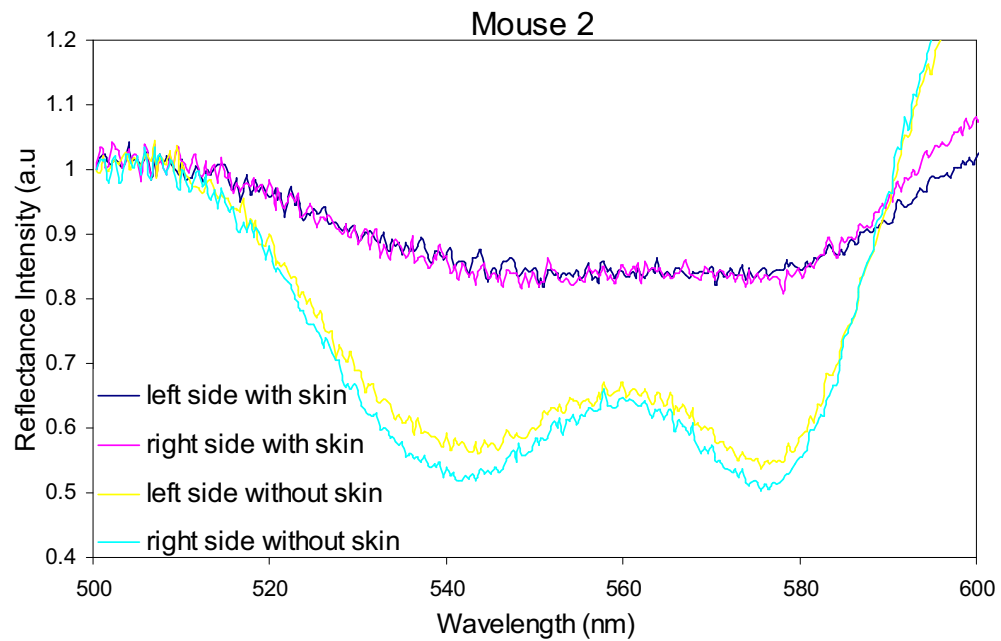


Figure 3.9 Optical reflectance curves obtained from the second P39 mouse with and without the skin at the site of measurement

3.3 Algorithm for oxygen saturation calculation

The algorithm used to quantify the concentration of hemoglobin (HbO and Hb) and oxygen saturation uses the mathematical model developed by Zonios and Dimou [33]. This model gives an expression relating the optical reflectance measured with a short source-detector separation optical probe, $R_p(\lambda)$, to the reduced scattering coefficient $\mu_s'(\lambda)$ and the absorption coefficient $\mu_a(\lambda)$ of the medium, as shown below:

$$R_p(\lambda) = [\mu_s'(\lambda)] / [k_1 + k_2(\mu_a(\lambda))] \quad \text{----- equation (2)}$$

The parameters k_1 and k_2 are calibrated using intralipid-blood tissue phantoms, since these parameters are unique for every optical probe and depends on the refractive indices of the tissue and the surrounding medium. Intralipid solution was used since it has optical properties similar to that of biological tissues [34]. The reduced scattering coefficient $\mu_s'(\lambda)$ and the absorption coefficient $\mu_a(\lambda)$ depend on the concentrations of HbO, Hb, melanin and water, and can be written as:

$$\mu_a(\lambda) = [\text{HbO}] \epsilon_{\text{HbO}}(\lambda) + [\text{Hb}] \epsilon_{\text{Hb}}(\lambda) + \% \text{H}_2\text{O} \epsilon_{\text{H}_2\text{O}}(\lambda) + [\text{mel}] \epsilon_{\text{mel}}(\lambda) \quad \text{----- equation (3)}$$

Here ' λ ' is the wavelength in nanometers (nm), $\epsilon_{\text{HbO}}(\lambda)$, $\epsilon_{\text{Hb}}(\lambda)$, $\epsilon_{\text{H}_2\text{O}}(\lambda)$, $\epsilon_{\text{mel}}(\lambda)$ are the extinction coefficients of HbO, Hb, water and melanin respectively. $[\text{HbO}]$, $[\text{Hb}]$, $[\text{mel}]$ are the concentrations of HbO, Hb and melanin.

$$\mu_s'(\lambda) = \{1 - [(\sqrt{d_0}) \lambda - \lambda_{\min} / (\sqrt{d_s}) \lambda_{\max} - \lambda_{\min}]\} \mu_s'(\lambda_{\min}) \quad \text{-----equation (4)}$$

Here d_s is the effective scatter size and d_0 is the effective scatter size at λ_{\min} [28]. From the tissue phantom measurements the values of μ_a and μ_s at two wavelengths (750nm and 830nm) were obtained using the ISS oximeter. The value of $\mu_s'(\lambda)$ was calculated using Mie theory, which is given as $\mu_s' = \mu_s (1-g)$ and $\mu_a(\lambda)$ was calculated using the extinction coefficients and chromophore concentrations as given in equation (3). After evaluating the values of $\mu_s'(\lambda)$ and $\mu_a(\lambda)$ the values k_1 and k_2 can be determined using equation (2), by getting a least squares fit line that best fits the plot of $[\mu_s'(\lambda) / R_p(\lambda)]$ vs $\mu_a(\lambda)$ [29]. After calculations the value of k_1 and k_2 for the optical probe used in this study was found to be 13.33 and 5.88 respectively. Using these k_1 and k_2 parameters, the measured reflectance spectra is given as the input to the

optimization algorithm which in turn quantifies the concentration of chromophores(HbO, Hb) and oxygen saturation by fitting the measured reflectance spectra with a 'fitted curve' using the least square analysis technique. An example of the fitted curve obtained from the optimization algorithm is shown below Figure 3.10.

The fitting parameters in the optimization algorithm include the absorption (concentration of Hb and HbO) and scattering coefficients, in Figure 3.10 the blue curve represents the measured reflectance spectra and the red curve represents the fitted curve.

Total hemoglobin concentration (HbT) is determined by adding the concentrations of HbO and Hb, i.e., $HbT = HbO + Hb$. The oxygen saturation percentage was determined using the following relation:

$$\text{Oxygen Saturation \%} = [HbO / HbT] \times 100$$

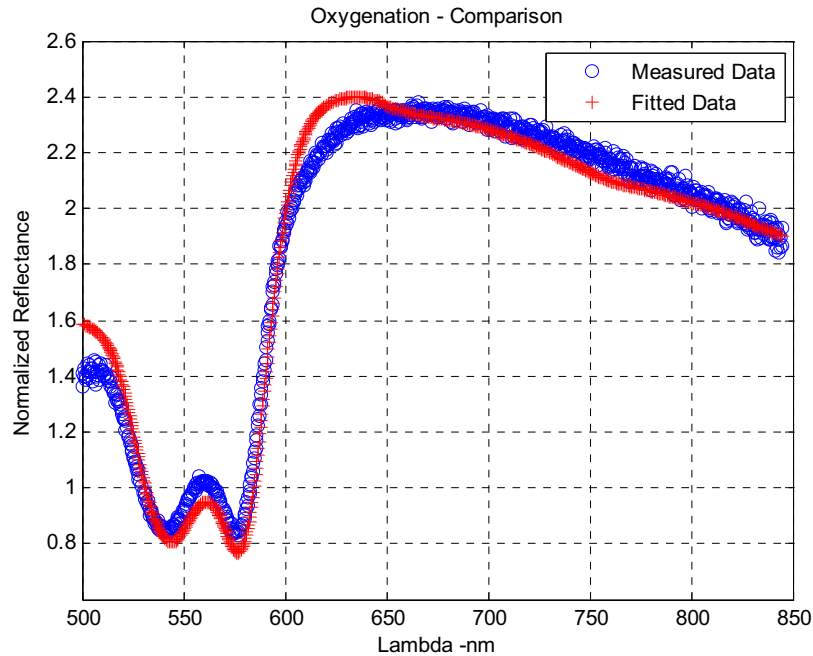


Figure 3.10 Illustration of the fitted curve obtained from the optimization algorithm

CHAPTER 4

RESULTS

All the data are expressed as mean concentrations obtained from all mice (in air or 100% oxygen group) \pm standard error mean (SEM). The concentrations of HbO, Hb, HbT and the oxygen saturation value during injury (8% oxygen) is given as a mean of their values from mice in both air and hyperoxia groups recorded during injury. Statistical comparison was done using student's t-test between the group of mice recovered in air and the group of mice recovered in 100% oxygen. P-value <0.05 was considered statistically significant.

4.1 Results obtained from P7 mice

This group had a total of 8 mice. The number of mice recovered in room air (air group) was 3 and the number of mice recovered in hyperoxia (hyperoxia group) was 5. The following concentrations of HbO, Hb, HbT (total hemoglobin) and oxygen saturation were obtained after analyzing of the recorded data using the optimization algorithm. The results obtained for this group is shown below:

Figure 4.1 shows that the concentration of HbO is very low during injury (8% oxygen) in both the left side (normal side) and the right side (injured side) of the brain. The concentration of HbO during recovery in hyperoxia is higher than that of recovery in air for the left side, but there was no significant difference since the p-value was found to be 0.11. In the injured side too, the concentration of HbO was higher in hyperoxia group when compared to that of air group; here too there was no significant difference. The p-value between the air and hyperoxia group for the right side was found to be 0.3.

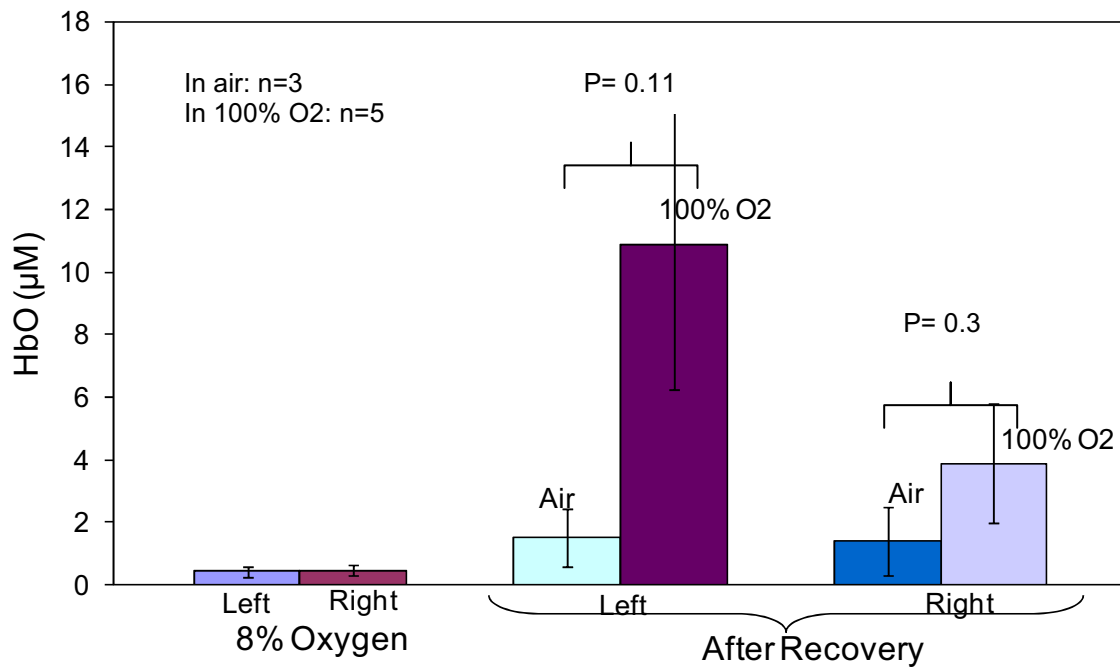


Figure 4.1 Concentration of oxy-hemoglobin for P7 mice during hypoxic ischemia and recovery in room air and 100% oxygen

Figure 4.2 shows the comparison of concentration of Hb between the air and hyperoxia group. The concentration of Hb in the injured side was found to be greater in the group recovered in hyperoxia when compared to the group recovered in room air. The p-value between them was found to be 0.08 indicating no significant difference between them. The p-value on the left side between the two groups was found to be 0.94. The concentration of Hb during hypoxia on both sides and its concentration on the normal side during recovery were found to be almost the same.

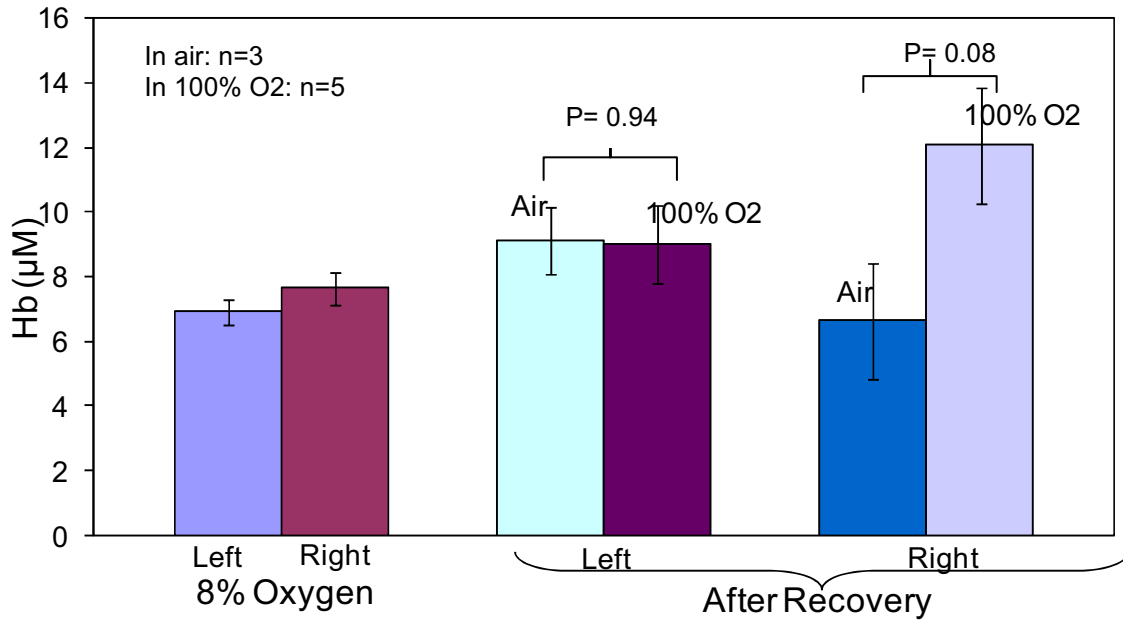


Figure 4.2 Concentration of de-oxy hemoglobin for P7 mice during hypoxic ischemia and recovery in room air and 100% oxygen

Figure 4.3 shows the comparison of concentration of HbT between the air and hyperoxia group. Mice recovered in air after injury showed a lower concentration of HbT on the injured side when compared to mice recovered in hyperoxia and their p-value was found to be 0.13. The p-value between the two groups for the normal left side of the brain tissue was found to be 0.16.

Similarly the oxygen saturation Figure 4.4 was also found to be lower in the group of mice recovered in room air when compared to that of hyperoxia, in the injured side. However there was no significant difference between them since p-value was 0.42. For the normal left side of the mouse brain the p-value between the two groups was found to be 0.04.

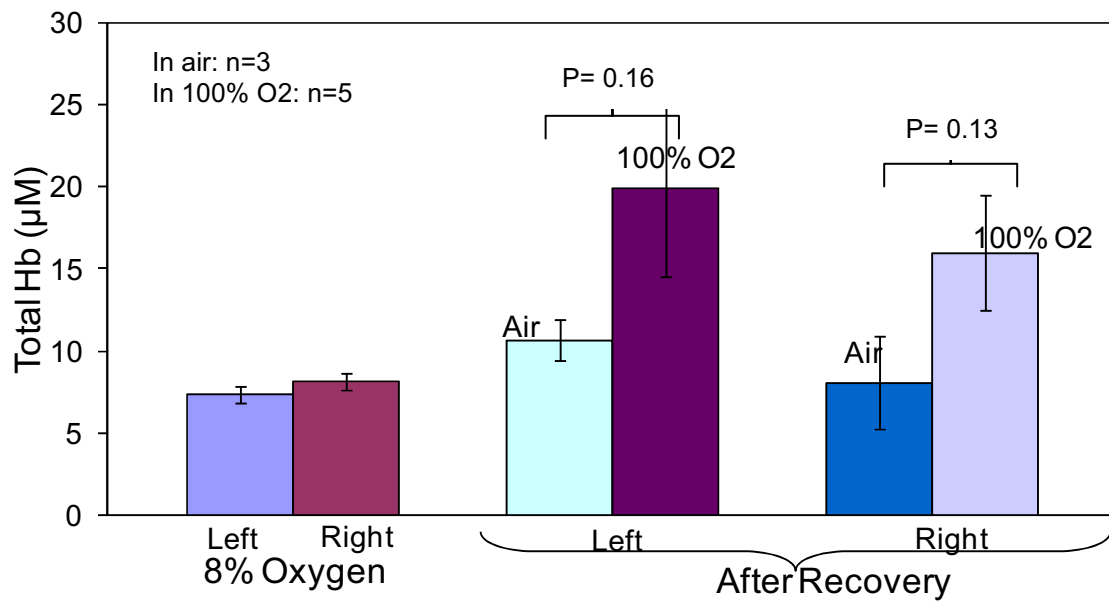


Figure 4.3 Concentration of Total hemoglobin for P7 mice during hypoxic ischemia and recovery in room air and 100% oxygen

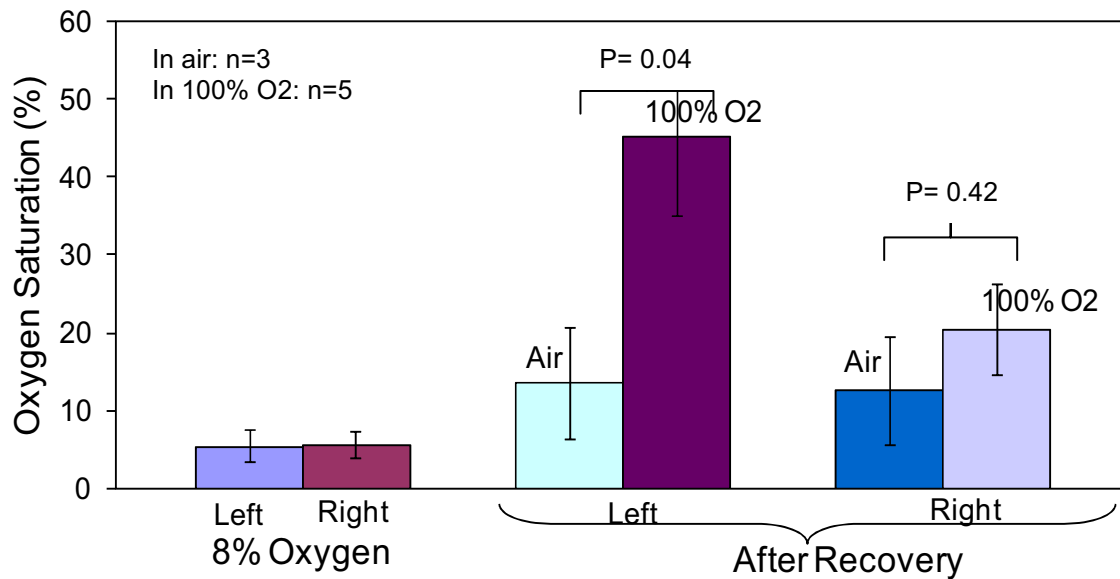


Figure 4.4 Comparison of oxygen saturation for P7 mice during hypoxic ischemia and recovery in room air and 100% oxygen

4.2 Results obtained from P14 mice

This group had a total of 9 mice. There were 5 mice in the air group and 4 mice in the hyperoxia group. Figure 4.5 shows that the concentration of HbO is much higher when ischemic mice was recovered in hyperoxia than when recovered in room air, the p-value was found to be 0.018 and 8.39E-05 (between recovery in air and hyperoxia) for the left and right side respectively showing a significant difference. HbO concentration during hypoxia is lower in both the sides and the injured side shows a lower concentration when compared to that of the left side due to focal ischemia.

The concentration of Hb shown in Figure 4.6 was higher in the air group both in the left and right side and has a p-value of 0.048 and 0.087 respectively, when compared with hyperoxia group.

Similarly the concentration of HbT shown in Figure 4.7 was higher in the hyperoxia group than in the air group for both left and right side, though significant differences could not be seen. The p-value between the two groups for the left and right side was found to be 0.35 and 0.32 respectively.

The oxygen saturation comparison shown in Figure 4.8 was much higher for mice recovered in hyperoxia in both the left and right side. The p-values between the air and hyperoxia group for the normal side was found to be 0.004 and for the injured side it was found to be 7.87E-05 indicating a significant difference.

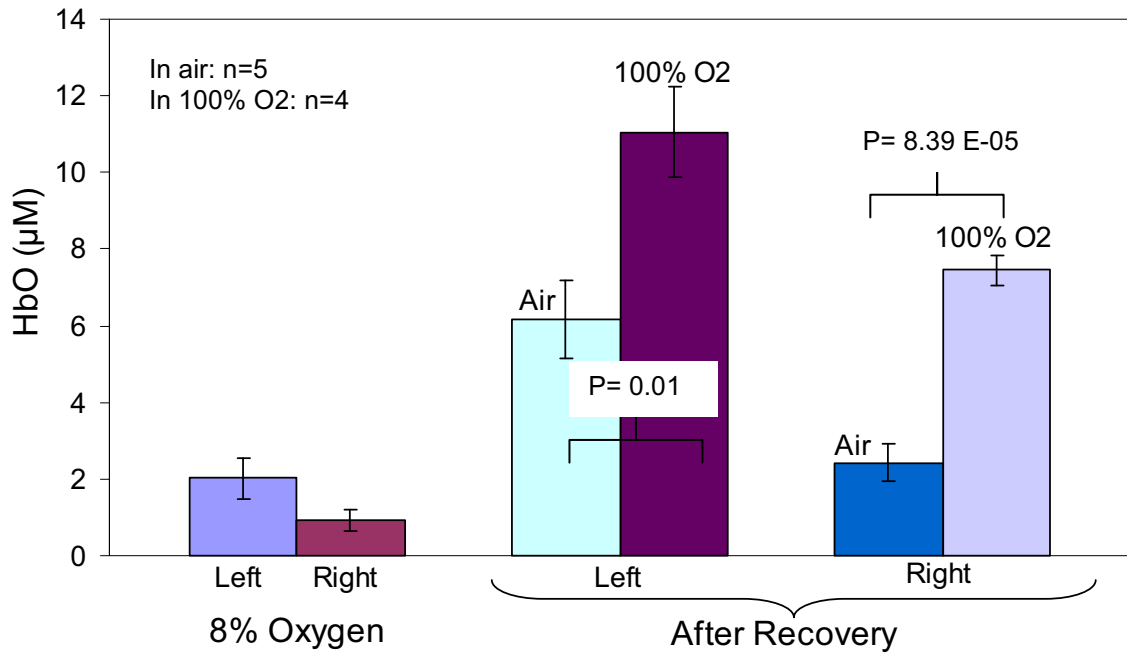


Figure 4.5 Concentration of oxy hemoglobin for P14 mice during hypoxic ischemia and recovery in room air and 100% oxygen

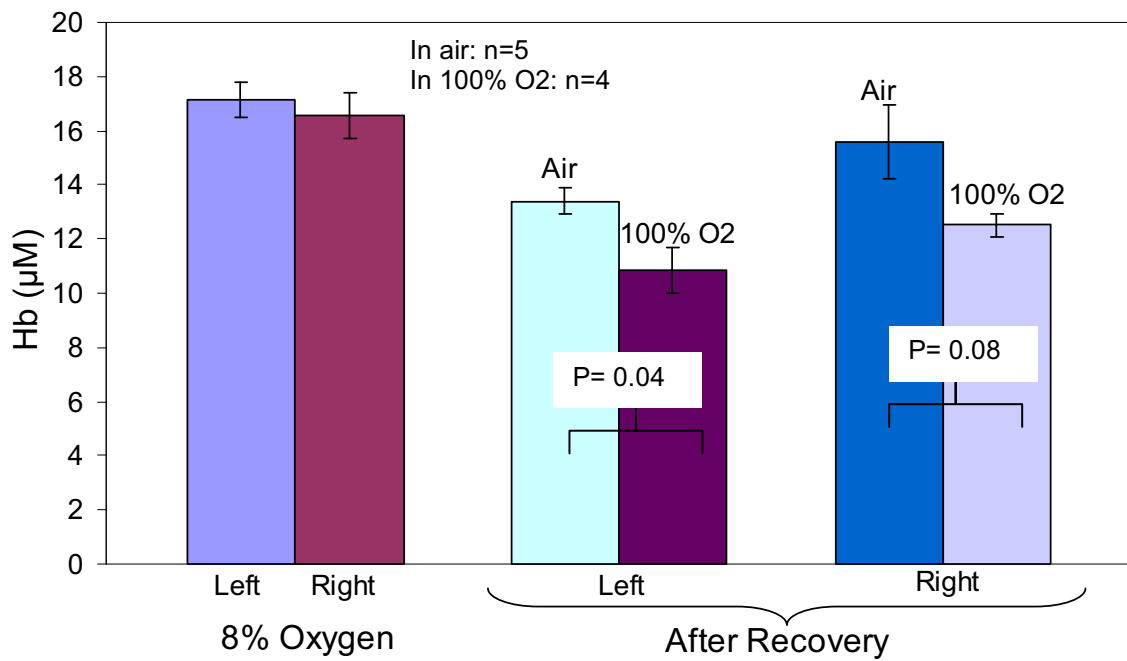


Figure 4.6 Concentration of de-oxy hemoglobin for P14 mice during hypoxic ischemia and recovery in room air and 100% oxygen

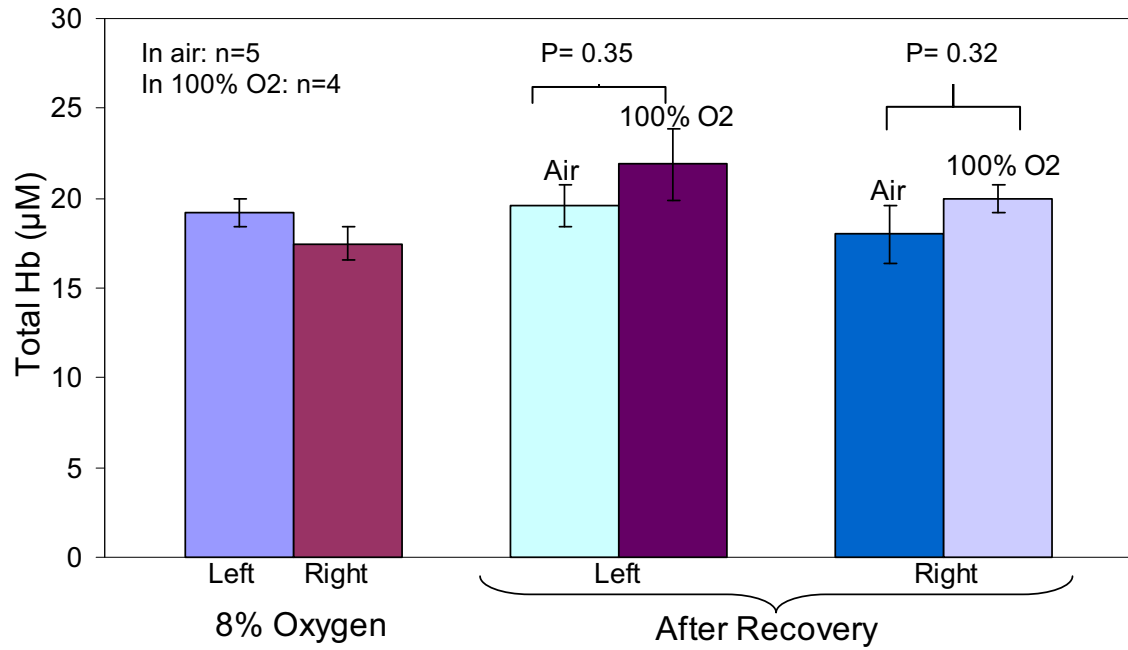


Figure 4.7 Concentration of total hemoglobin for P14 mice during hypoxic ischemia and recovery in room air and 100% oxygen

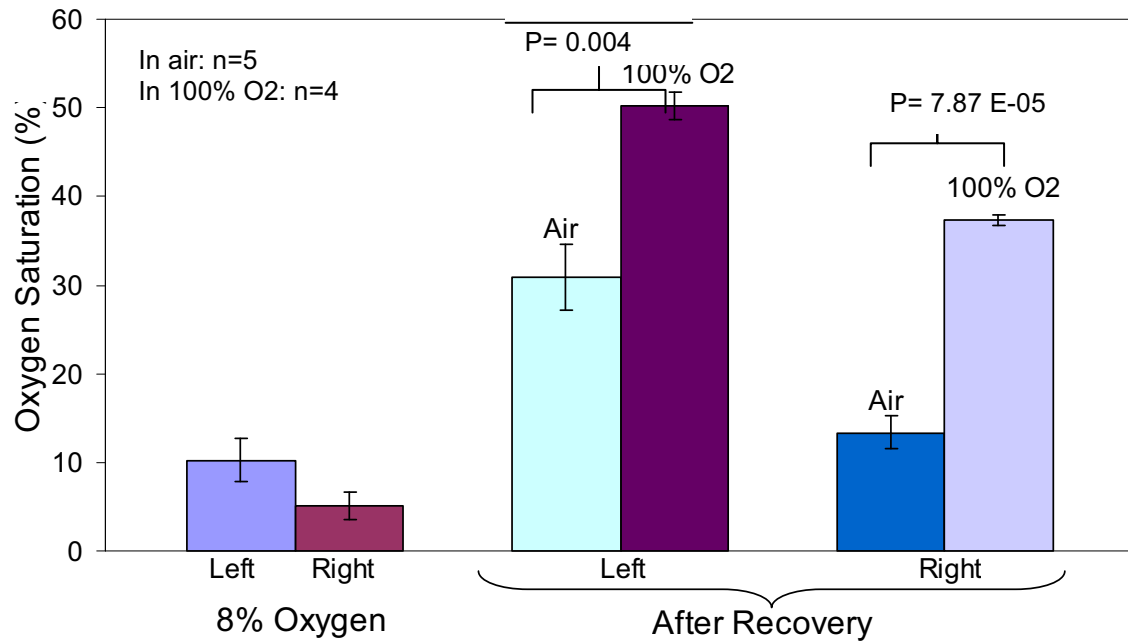


Figure 4.8 Comparison of oxygen saturation for P14 mice during hypoxic ischemia and recovery in room air and 100% oxygen

4.3 Results obtained from P21 mice

This group had a total of 10 mice. There were 5 mice in the air group and 5 mice in the hyperoxia group. The concentration of HbO shown in Figure 4.9 was a little higher in mice recovered in hyperoxia than mice recovered in air, for the injured side. However it was not significantly different, with a p-value of 0.177. The p-value between the two groups for the normal side was 0.02.

The concentration of Hb, Figure 4.10 and HbT shown in Figure 4.11 also do not show any significant difference between recovery in air and hyperoxia. The p-value between the two groups for the left and right side was found to be 0.92 and 0.34 respectively for Hb concentration.

The p-value between the two groups for the left and right side was found to be 0.08 and 0.76 respectively for HbT concentration.

Oxygen saturation shown in Figure 4.12 was higher in both left and right side during recovery in hyperoxia when compared to recovery in air. Significant difference was seen only in the left side, having a p-value of 0.015. The right side showed a p-value of 0.11.

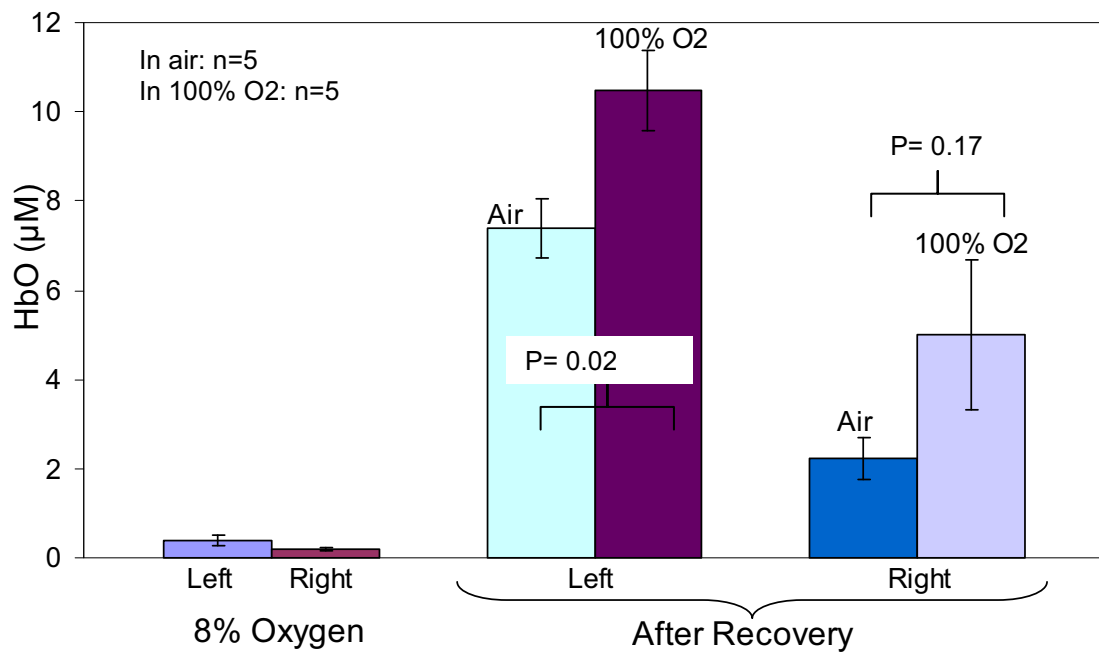


Figure 4.9 Concentration of oxy hemoglobin for P21 mice during hypoxic ischemia and recovery in room air and 100% oxygen

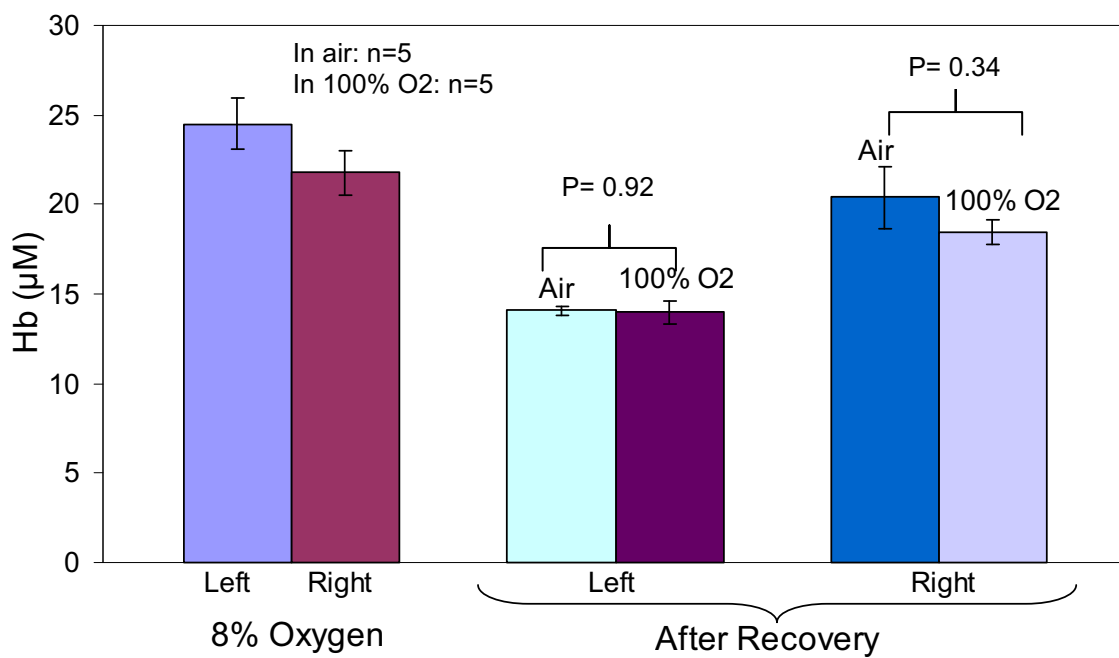


Figure 4.10 Concentration of de-oxy hemoglobin for P21 mice during hypoxic ischemia and recovery in room air and 100% oxygen

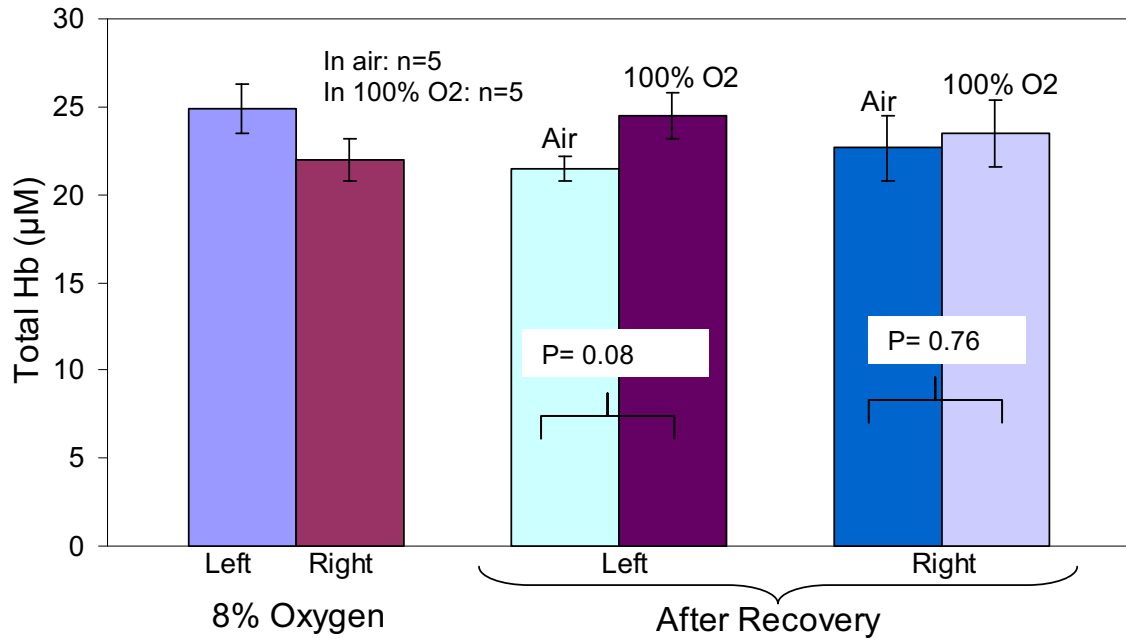


Figure 4.11 Concentration of total hemoglobin for P21 mice during hypoxic ischemia and recovery in room air and 100% oxygen

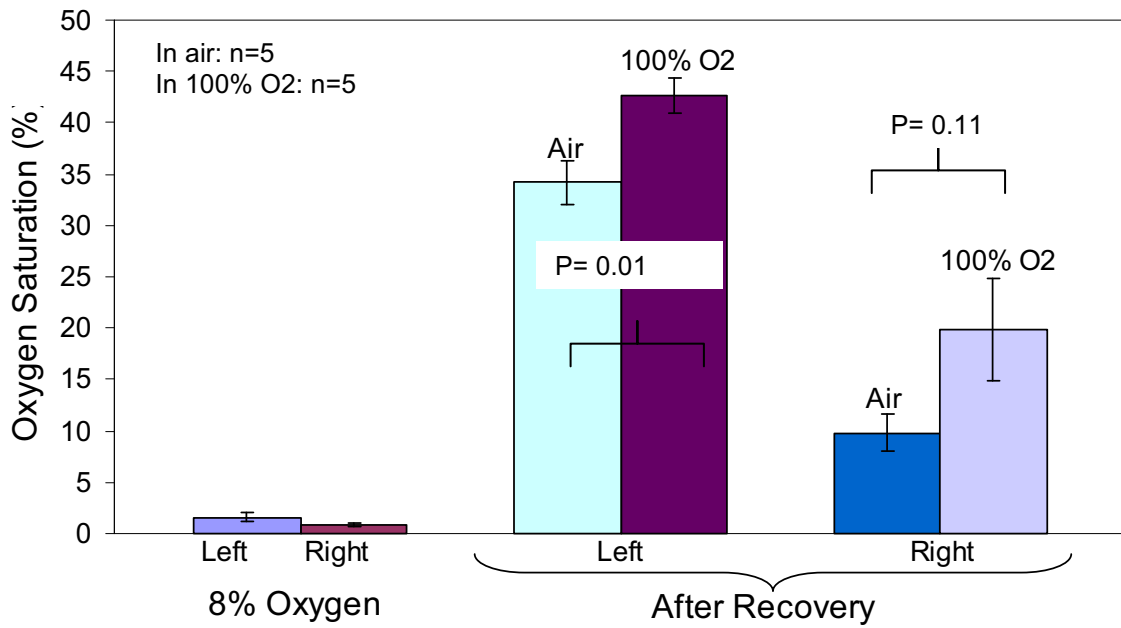


Figure 4.12 Comparison of oxygen saturation for P21 mice during hypoxic ischemia and recovery in room air and 100% oxygen

4.4 Results obtained from P28 mice

This group had a total of 6 mice. Three mice recovered in room air after injury and 3 mice recovered in hyperoxia. The concentration of HbO shown in Figure 4.13 was higher in mice recovered in hyperoxia than mice recovered in air, for the injured side. However it was not significantly different, with a p-value of 0.28. The normal side showed a higher concentration of HbO in the air group than in the hyperoxia group, but the p-value was 0.5 and hence not significantly different.

The concentration of Hb, Figure 4.14 and HbT shown in Figure 4.15 also do not show any significant difference between recovery in air and hyperoxia for the injured side although their values in the hyperoxia group is much higher than that of air group. The p-value between the two groups for the left and right side was found to be 0.83 and 0.13 respectively for Hb concentration.

The p-value between the two groups for the left and right side was found to be 0.32 and 0.16 respectively for HbT concentration.

Oxygen saturation shown in Figure 4.16 was almost the same for both air and hyperoxia groups in the left as well as the right side. No significant difference between them could be seen. The p-value between the two groups for the left and right side was found to be 0.73 and 0.65 respectively.

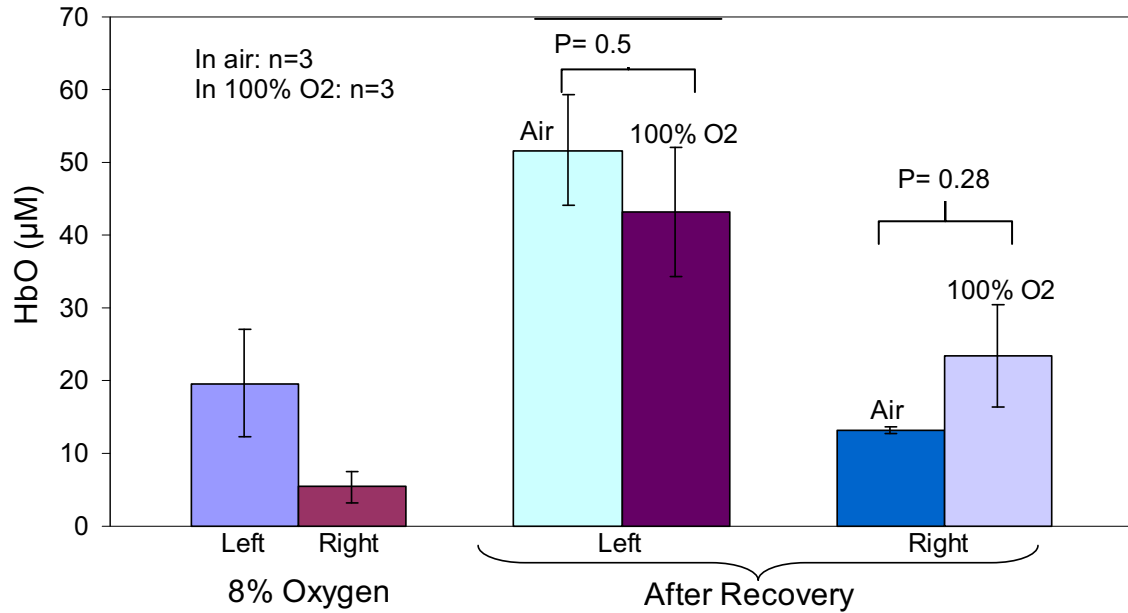


Figure 4.13 Concentration of oxy hemoglobin for P28 mice during hypoxic ischemia and recovery in room air and 100% oxygen

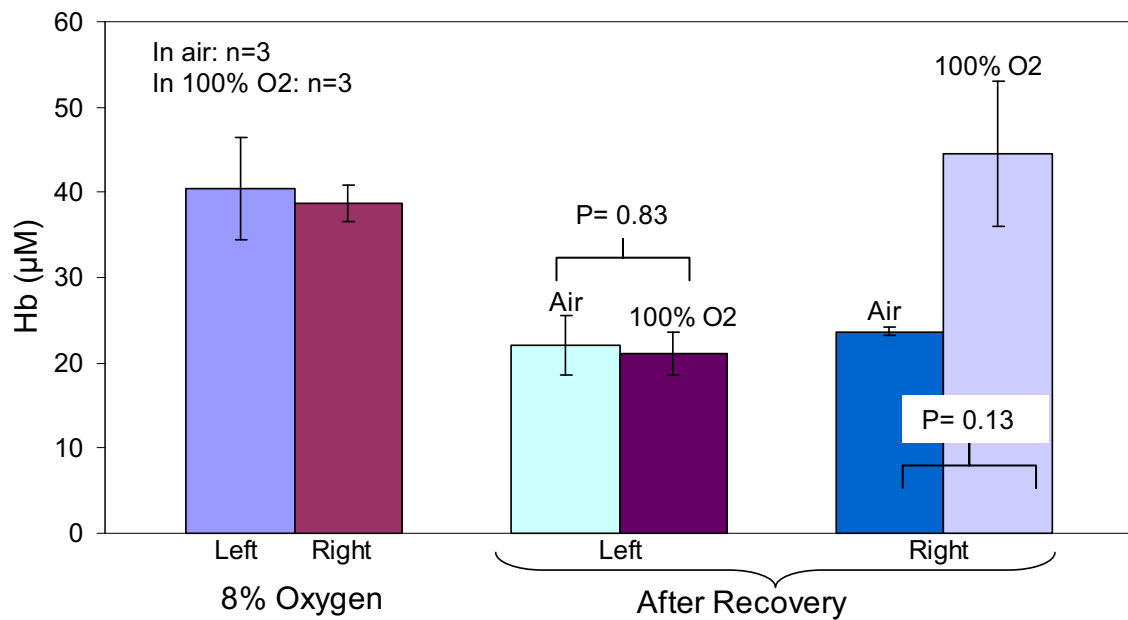


Figure 4.14 Concentration of de-oxy hemoglobin for P28 mice during hypoxic ischemia and recovery in room air and 100% oxygen

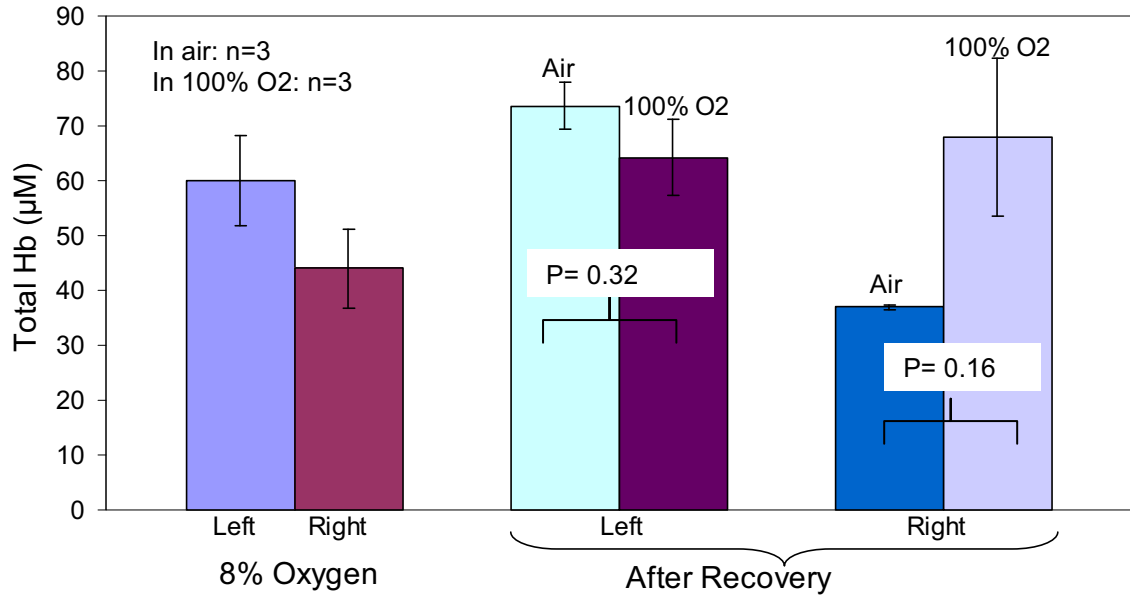


Figure 4.15 Concentration of total hemoglobin for P28 mice during hypoxic ischemia and recovery in room air and 100% oxygen

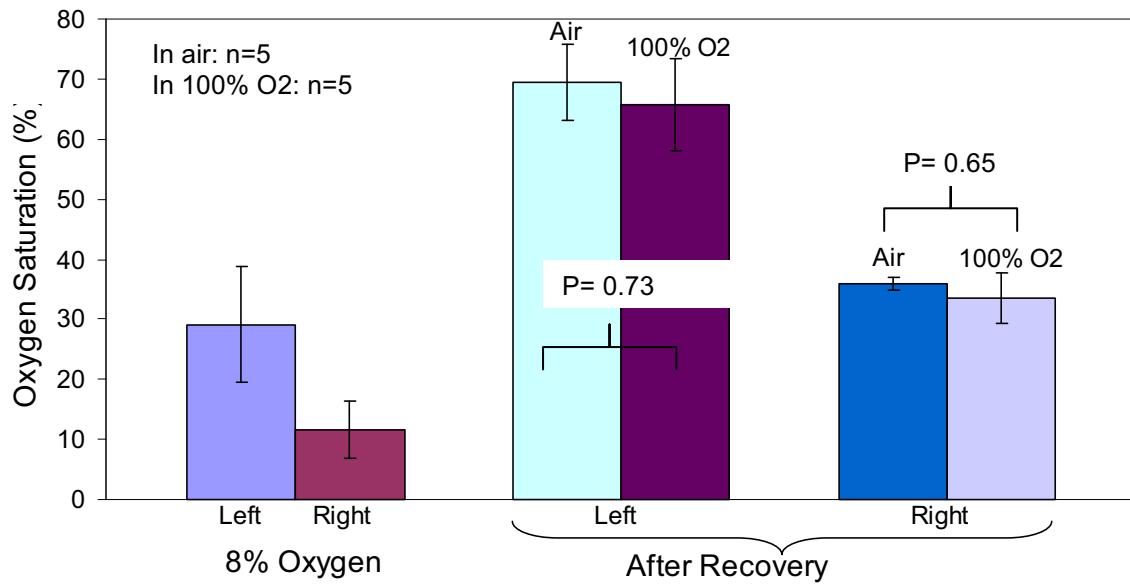


Figure 4.16 Comparison of oxygen saturation for P28 mice during hypoxic ischemia and recovery in room air and 100% oxygen

4.5 Results obtained from P60 mice

This group had a total of 15 mice. Seven mice recovered in room air and eight mice recovered in hyperoxia after the injury. The concentration of HbO Figure 4.17, concentration of HbT Figure 4.19, and oxygen saturation Figure 4.20 are higher when the injured mice are recovered in hyperoxia when compared to mice recovered in air. No significant difference could be seen, since the p-value was >0.05 . Concentration of Hb Figure 4.18 was found to be higher on both left and right side for mice recovered in air when compared to mice recovered in hyperoxia.

The p-values obtained between the two groups for the left and right side was 0.2 and 0.16 for HbO concentration respectively. The p-values obtained between the two groups for the left and right side was 0.07 and 0.6 for Hb concentration respectively.

The p-values obtained between the two groups for the left and right side was 0.35 and 0.36 for HbT concentration respectively. The p-values obtained between the two groups for the left and right side was 0.07 and 0.06 for oxygen saturation respectively.

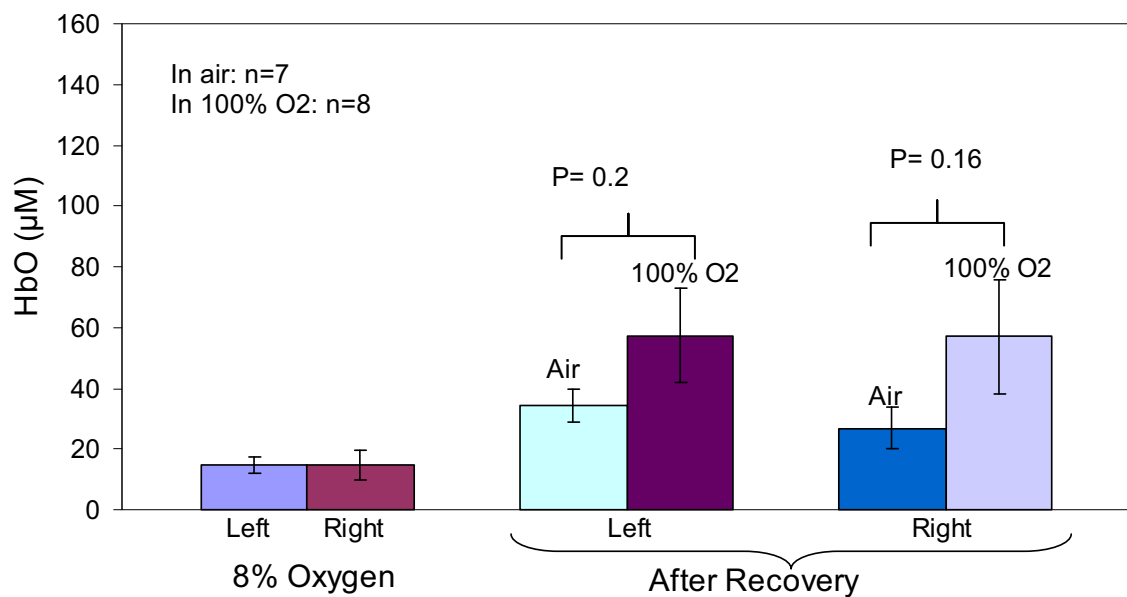


Figure 4.17 Concentration of oxy hemoglobin for P60 mice during hypoxic ischemia and recovery in room air and 100% oxygen

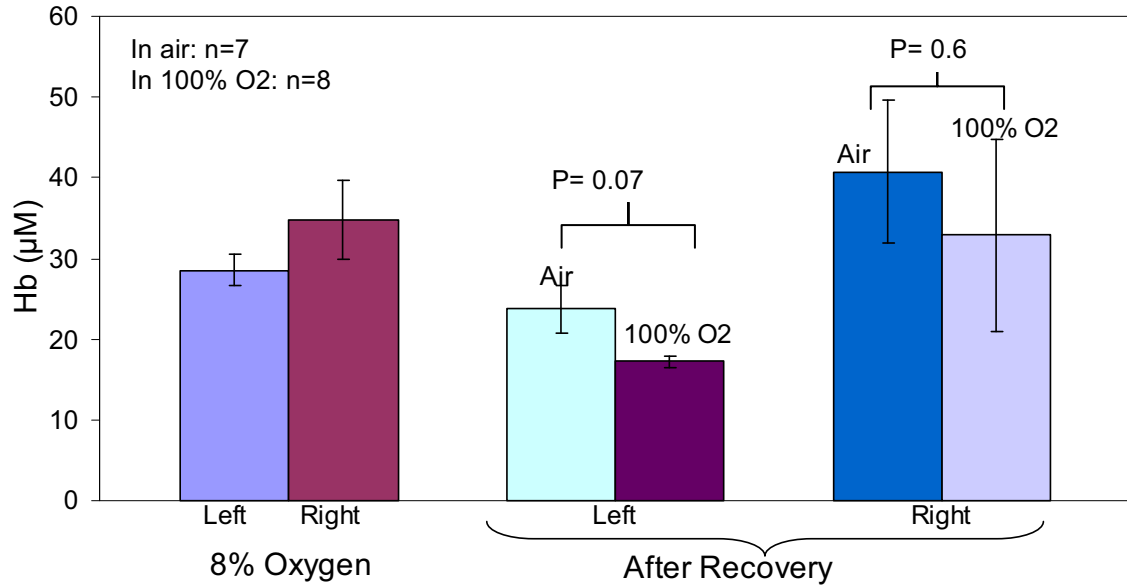


Figure 4.18 Concentration of de-oxy hemoglobin for P60 mice during hypoxic ischemia and recovery in room air and 100% oxygen

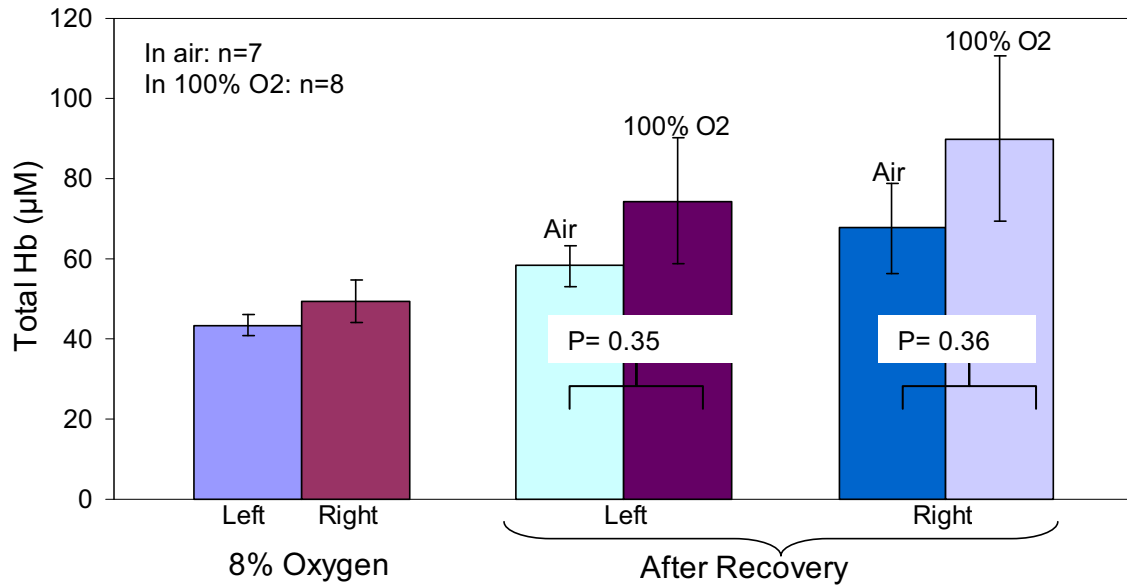


Figure 4.19 Concentration of total hemoglobin for P60 mice during hypoxic ischemia and recovery in room air and 100% oxygen

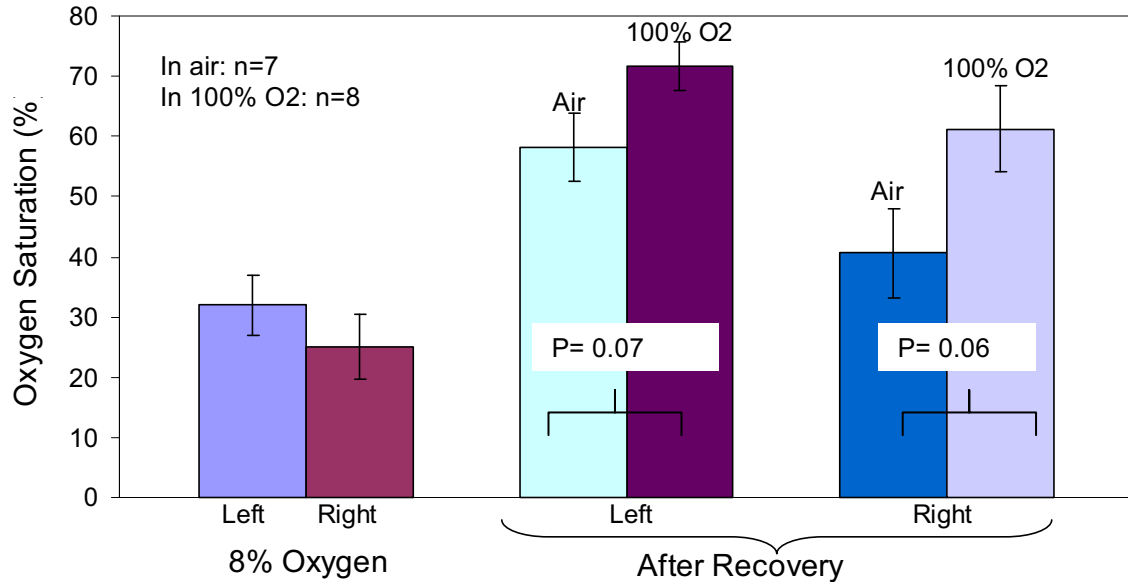


Figure 4.20 Comparison of oxygen saturation for P60 mice during hypoxic ischemia and recovery in room air and 100% oxygen

4.6 Age related comparison of HbO and oxygen saturation

Figure 4.21 shows that the concentration of HbO on the right (injured) side was higher when mice were recovered in normobaric hyperoxia than when it was recovered in room air. Comparison is done between age groups P7, P28 and P60 together, since all mice in these groups had their skin removed at the site of measurement. Figure 4.22 shows that even the oxygen saturation was higher (except in P28 group) when mice were recovered in normobaric hyperoxia than when recovered in room air.

Effect of recovery after treatment with air and normobaric hyperoxia at different developmental stages of the brain seems to vary. When the concentration of oxyhemoglobin and oxygen saturation was compared between the different age groups in Figure 4.21 and 4.22, significant difference between P7 and P60 group was observed. However a recent study has shown that administering normobaric hyperoxia after brain injury can damage the tissue since it causes an increase in free radical production and it in fact exacerbates the injury and impairs functional recovery in neonatal mice [39]. The study proves that the extent of histological brain

injury in young mice after hypoxic ischemic brain injury when recovered in normobaric hyperoxia is higher when compared to that of older mice. Enzymes and antioxidants required for neural protection against free radical injury are present in significantly less amounts in young mice brain tissue when compared to the mature mouse brain. Reduced protective enzymes and antioxidants in the immature brain make it vulnerable to oxidative injury during recovery in hyperoxia [39]. This might be one of the reasons for the significant difference observed between the two groups (P7 and P60) after recovery in normobaric hyperoxia.

Also when HbO concentration and oxygen saturation values of p28 and p60 groups were compared, significant difference in oxygen saturation values between the two groups could only be observed on the right (injured) side when recovered in normobaric hyperoxia (not shown in figure). Similar results were obtained when P14 and p21 groups were compared. These two groups (p14 and p21) were not compared with P7, P28 and P60 groups since measurements were obtained from them without removing the skin at the site of measurement. Significant difference in oxygen saturation values between the P14 and P21 groups could only be observed on the right (injured) side when recovered in normobaric hyperoxia.

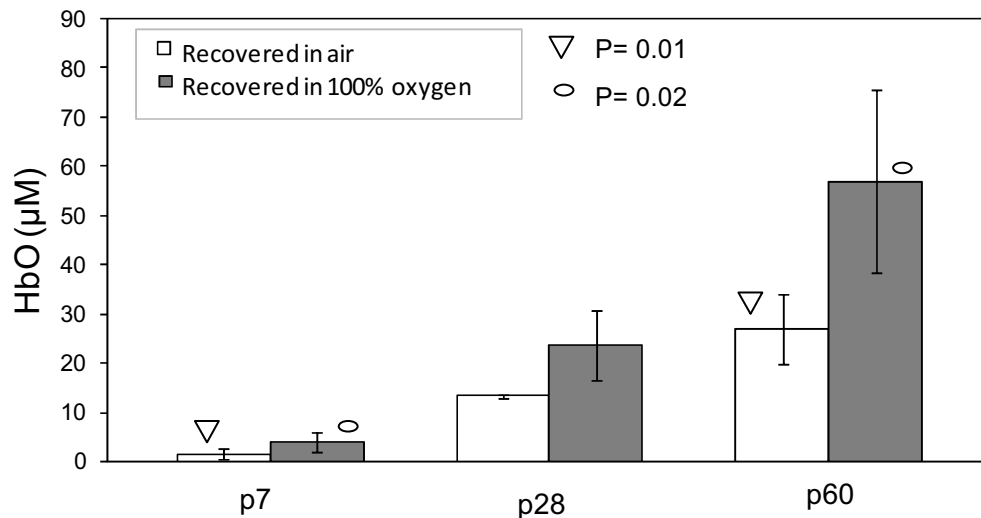


Figure 4.21 Comparison of oxyhemoglobin concentration on the right (injured) side between all mice in P7, P28 and P60 groups after recovery in room air and 100% oxygen

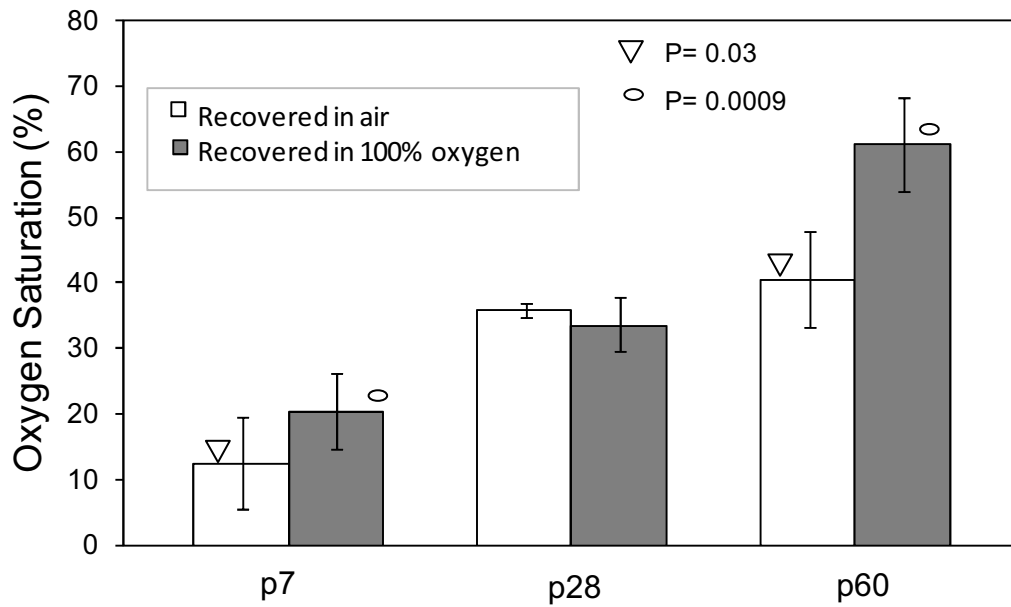


Figure 4.22 Comparison of oxygen saturation on the right (injured) side between all mice in P7, P28 and P60 groups after recovery in room air and 100% oxygen

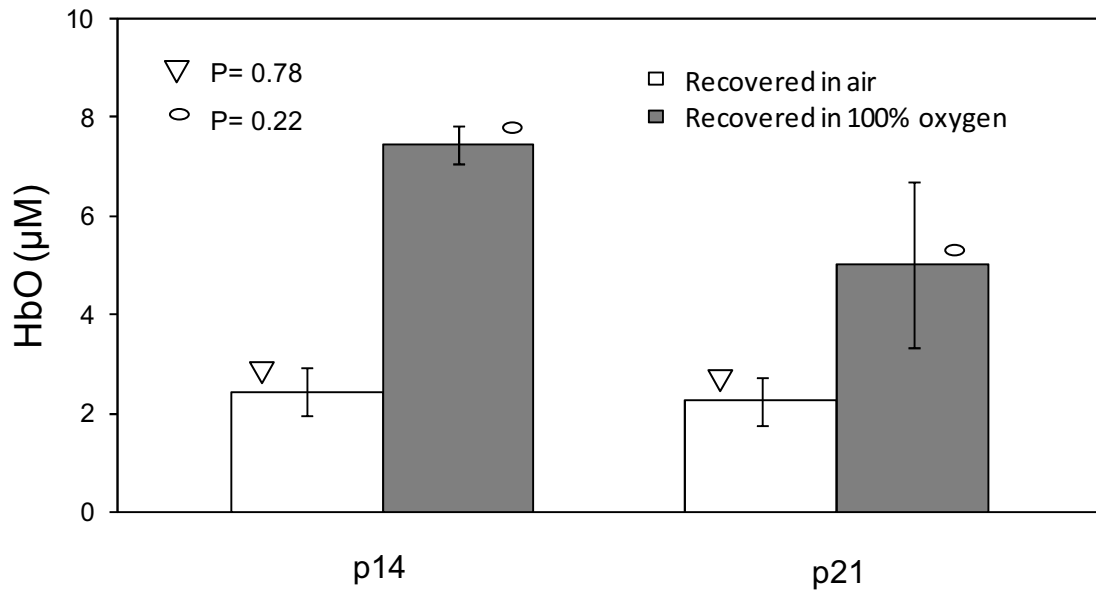


Figure 4.23 Comparison of oxyhemoglobin concentration on the right (injured) side between all mice in P14 and P21 groups after recovery in room air and 100% oxygen

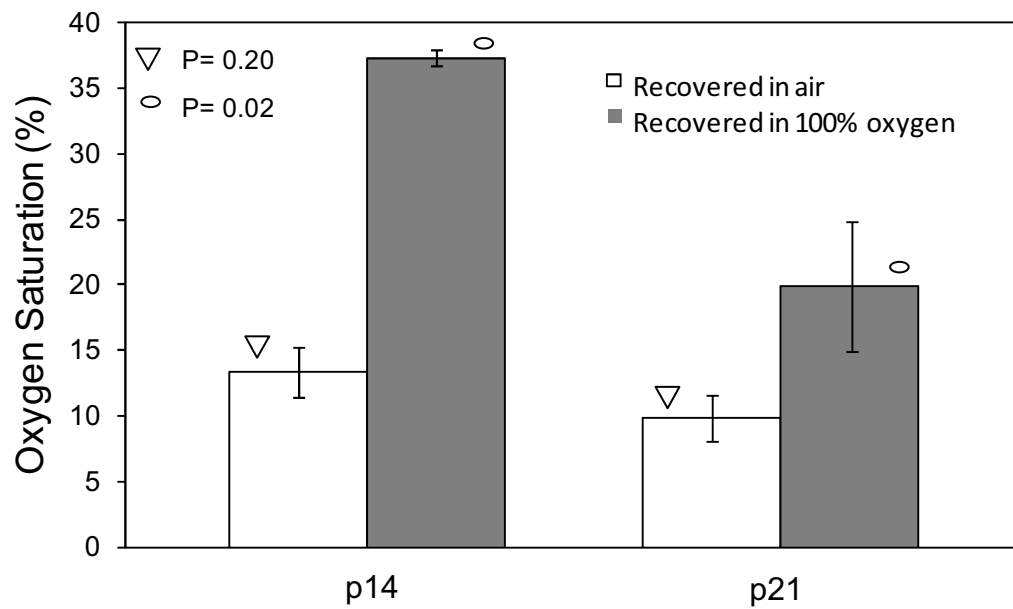


Figure 4.24 Comparison of oxygen saturation on the right (injured) side between all mice in P14 and P21 groups after recovery in room air and 100% oxygen

CHAPTER 5

DISCUSSION AND FUTURE WORK

The goal of this study was to determine the concentration of hemoglobin (HbO and Hb), and oxygen saturation of mice with focal hypoxia-ischemic injury, using optical spectroscopy measurements, and to determine how their concentrations varied when these mice were recovered in room air and recovered in normobaric hyperoxia.

Reduced blood flow after a stroke causes oxygen decrease in the brain tissue, thereby damaging the tissue. Oxygen therapy for ischemic stroke can be beneficial; however some potential harmful effects of this therapy for ischemic stroke raises concern due to oxygen free radical injury and the possibility of cerebral vasoconstriction if hyperoxia is administered to the ischemic tissue which could further reduce the oxygen supply to the damaged tissue thereby worsening the stroke outcome. Hence it is important to study the effects of normobaric hyperoxia treatment for focal cerebral ischemia in the ischemic as well as non ischemic tissues.

The results presented in this thesis shows that mice recovered in hyperoxia improves the concentration of oxyhemoglobin in the injured side when compared with the mice recovered in room air, for all the age groups. As expected, HbO concentrations and oxygen saturation were reduced during hypoxia in all groups of mice. The ligation of the right carotid artery followed by hypoxia, highly reduced the concentration of oxyhemoglobin and oxygen saturation on the ipsilateral side due to ischemic injury.

Observed low levels of HbO concentration and oxygen saturation on the (normal/contralateral) left side of the brain tissue maybe due to moderate hypoperfusion [35]. The oxygen saturation increased in the left side of the brain in all groups of mice when recovered in normobaric hyperoxia, due to its non ligated vasculature and increase in oxygen concentration when breathing 100% oxygen. Although the free radical generation was not

directly measured, it is known that oxygen free radicals cause damage to the cell membranes thereby injuring the tissue even further. The neuroprotection of the ischemic tissue by recovery in normobaric hyperoxia was presumed, and the increased concentration of HbO and oxygen saturation supports this presumption. Since the injured right side lacks open vasculature due to carotid artery ligation, the increase in HbO concentration and oxygen saturation might reflect an already established collateral vasculature [36]. This increase in oxygen delivery to the ischemic neurons and glia improves the oxidative metabolism. These results are supported by a prior study which showed that normobaric hyperoxia improved both cerebral oxygenation and blood flow in mice with focal cerebral ischemia [37,38].

The age of the mice also seem to influence the concentration of HbO and oxygenation in the ischemic tissue when recovered in normobaric hyperoxia. Further studies are required to investigate this behavior and to correlate it with human measurements. Further studies can also be done to learn the impact of normobaric hyperoxia on the infarct size, and blood flow in the ischemic tissue. Also the sample size can be increased in each age group of mice to increase the power of these conclusions and verify the results.

REFERENCES

1. Stroke: Hope through research," NINDS. Publication date July 2004, NIH publication No. 99-2222
2. www.nlm.nih.gov/medlineplus/stroke.html
3. www.merck.com
4. www.ohsu.edu/xd/
5. www.strokeassociation.org
6. www.strokecenter.org
7. www.ninds.nih.gov
8. Pang Z et al., Acute excitotoxic necrosis and delayed apoptosis. J. Neurosci. 1997 May ;17 (9):3064-73.
9. www.wikipedia.com
10. Yin et al., Inhibition of apoptosis by hyperbaric oxygen in a rat focal cerebral ischemic model. Journal of cerebral blood flow and metabolism 23, 855-864.
11. John H Z et al., Mechanism of hyperbaric oxygen and neuroprotection in stroke. Elsevier pathophysiology 12(2005) 65-80.
12. Knighton DR et al., Oxygen tension regulates the expression of angiogenesis factor by macrophages. Pubmed PMID 6612342.
13. David A. Steenblock , A Brief review of hyperbaric oxygen for stroke rehabilitation.
14. R.M. Leach et al. ABC of Oxygen: Hyperbaric oxygen therapy.
15. Anderson et al., A pilot study of hyperbaric oxygen in the treatment of human stroke. Pubmed PMID 1926256.
16. Rusyniak DE et al., Hyperbaric oxygen therapy in acute ischemic stroke: results of the hyperbaric oxygen in acute ischemic stroke trial pilot study. Pubmed PMID: 12574578.
17. Johns, Maureen, Giller, Cole A., Liu Hanli. Determination of hemoglobin oxygen saturation from turbid media using reflectance spectroscopy with small source-detector separations. Applied spectroscopy, Volume 55, Issue 12, Pages 388A-408A and 1573-1733 (December 2001), pp. 1686-1694(9) Society for applied spectroscopy.

18. Janet S.S. et al., Near-infrared spectroscopy. Seminars in pediatric neurology, Volume 6, Issue 2.
19. T. J. Germon *et al.*, *Cerebral near infrared spectroscopy: emitter-detector separation must be increased*. British Journal of Anaesthesia 82 (6): 831–7 (1999)
20. www.nirsoptix.com
21. David A. B. et al., Design of a visible-light spectroscopy clinical tissue oximeter. J Biomed Opt. 2005 Jul-Aug;10(4):44005.
22. Benaron DA. Et al., Continuous, noninvasive, and localized microvascular tissue oximetry using visible light spectroscopy. Anesthesiology. 2004 Jun;100(6):1469-75.
23. Amir G. et al., Visual light spectroscopy reflects flow-related changes in brain oxygenation during regional low-flow perfusion and deep hypothermic circulatory arrest. J Thorac Cardiovasc Surg. 2006 Dec;132(6):1307-13. Epub 2006 Nov 16.
24. Hoshino T. et al., Intraoperative monitoring of cerebral blood oxygenation and hemodynamics during extracranial-intracranial bypass surgery by a newly developed visible light spectroscopy system. Surg Neurol. 2006 Jun;65(6):569-76; discussion 576.
25. I. Tachtsidis, The technique of near-infrared spectroscopy.
26. <http://www.medphys.ucl.ac.uk>
27. Elwell CE. A practical users guide to near infrared spectroscopy.
28. Dheerendra K et al., Investigation of model parameters for short distance light reflectance and its application to study formalin-induced pain responses in rats. Optical society of America.
29. Aditya M. et al., Model-driven analysis of optical reflectance spectroscopy for detection of human prostate and kidney cancer.
30. Ulrika Ådén et al., MRI evaluation and functional assessment of brain injury after hypoxic ischemia in neonatal mice. (Stroke. 2002;33:1405.)
31. Sheldon RA. Et al., Strain-related brain injury in neonatal mice subjected to hypoxia-ischemia. Brain Res. 1998 Nov 9;810(1-2):114-22.
32. Radhakrishnan H. et al., Determination of hemoglobin oxygen saturation in rat sciatic nerve by in vivo near infrared spectroscopy. Brain Res. 2006 Jul 7;1098(1):86-93. Epub 2006 Jun 19.
33. G. Zonios and A. Dimou, "Modeling diffuse reflectance from semi-infinite turbid media: application to the study of skin optical properties". Opt Express 14, 8661-8674 (2006).
34. Staveren et al., Light scattering in Intralipid-10% in the wavelength range of 400-1100 nm. Optical society of America.

35. Dijkhuizen RM. et al., Dynamics of cerebral tissue injury and perfusion after temporary hypoxia-ischemia in the rat: evidence for region-specific sensitivity and delayed damage. *Stroke*. 1998 Mar;29(3):695-704.
36. Wei L. et al., Collateral growth and angiogenesis around cortical stroke. *Stroke*. 2001 Sep;32(9):2179-84.
37. H. K. Shin et al., Normobaric hyperoxia improves cerebral blood flow and oxygenation, and inhibits peri-infarct depolarizations in experimental focal ischemia. *Brain* (2007), 130, 1631-1642 Advance access publication.
38. Aneesh B.S. et al., Effects of normobaric hyperoxia in a rat model of focal cerebral ischemia–reperfusion. *Journal of cerebral blood flow & metabolism*.
39. Joshua D.K. et al., Brief exposure to hyperoxia depletes the glial progenitor pool and impairs functional recovery after hypoxic-ischemic brain injury. *Journal of cerebral blood flow & metabolism* (2008).

BIOGRAPHICAL INFORMATION

Shereen Mohideen was born on April 3rd, 1984 in Bangalore, India. She attended B.M.S. College of engineering in Bangalore from 2002 to 2006 and received her Bachelor of Engineering degree in Medical Electronics from Visvesvaraya Technological University, India in the year 2006. Her research interests include medical imaging and biomedical instrumentation.

In fall 2006, she started her graduate studies (M.S. course) in Biomedical Engineering from a Joint Program of Biomedical Engineering at the University of Texas at Arlington and University of Texas Southwestern Medical Center at Dallas, completing it by summer 2008.